ESECMaSE

Enhanced **S**afety and **E**fficient **C**onstruction of **Ma**sonry **S**tructures in **E**urope

Project No. Coll – Ct - 2003 - 500291

ESECMaSE

Enhanced Safety and Efficient Construction of Masonry Structures in Europe

Horizontal Research Activities Involving SMEs

Collective Research

Work Package N°: 7

D 7.2a Test results on the earthquake resistance on improved masonry materials by pseudo dynamic tests

Prof. Dr.-Ing. E. Fehling, Dipl.-Ing. J. Stuerz, Dipl.-Ing. Eyad Aldoghaim

Due date of deliverable: 10.01.2008
Actual submission date: 29.02.2008

Start date of project: 10.04.2004 Duration: 36 months

University of Kassel
Institute of Structural Engineering
Chair of Structural Concrete
Kurt-Wolters-Straße 3
34125 Kassel [draft 1]

Project co-funded by the European Commission within the Sixth Framework Programme (2002-2006)		
Dissemination Level		
PU	Public	X
PP	Restricted to other programme participants (including the Commission Services)	
RE	Restricted to a group specified by the consortium (including the Commission Services)	
CO	Confidential, only for members of the consortium (including the Commission Services)	

Contents:

1. Introduction

Deliverable 7.2 of ESECMaSE deals with pseudo dynamic tests on masonry walls. Since the pseudo dynamic wall tests of the ESECMaSE project were carried out at two different laboratories, this deliverable is divided into two parts:

⇒ D 7.2a - University of Kassel (UNIK)

⇒ D 7.2b - Technical University of Munich (TUM)

This report describes the pseudo dynamic wall tests with a test set-up developed in WP 6 on different kinds of masonry (clay, calcium silicate) with different specimen dimensions, carried out at Kassel University.

2. Materials used

The first and the last layer of mortar of all tested walls were fabricated with a general purpose mortar Sakret ZM M10 according to DIN EN 998-2. The other kinds of mortar were specific to each kind of bricks.

2.1. Walls made of clay bricks

2.1.1. Units

Three different kinds of vertically perforated clay bricks were used. Two of them had a width of 175 mm and a length of 363 mm, the third one had a width of 300 mm and a length of 249 mm. The height of all used clay bricks was 248 mm, because they are used with thin layer mortar.

The optimised bricks had different hole patterns but the same density as a conventional clay brick HLZ-Plan–12–0.9–9DF (see [5] and [6]).

The confinement bricks were filled with an unreinforced concrete, which should have had the strength of a concrete C20/25. At the time of testing the wall the compressive strength of two concrete cubes was tested with an average strength of 51.6 N/mm^2.

The third brick was a Plan T10 – 30.0. This one had an allowable stress σ_0 of 0.7 N/mm2 according to approval Z-17.1-889.

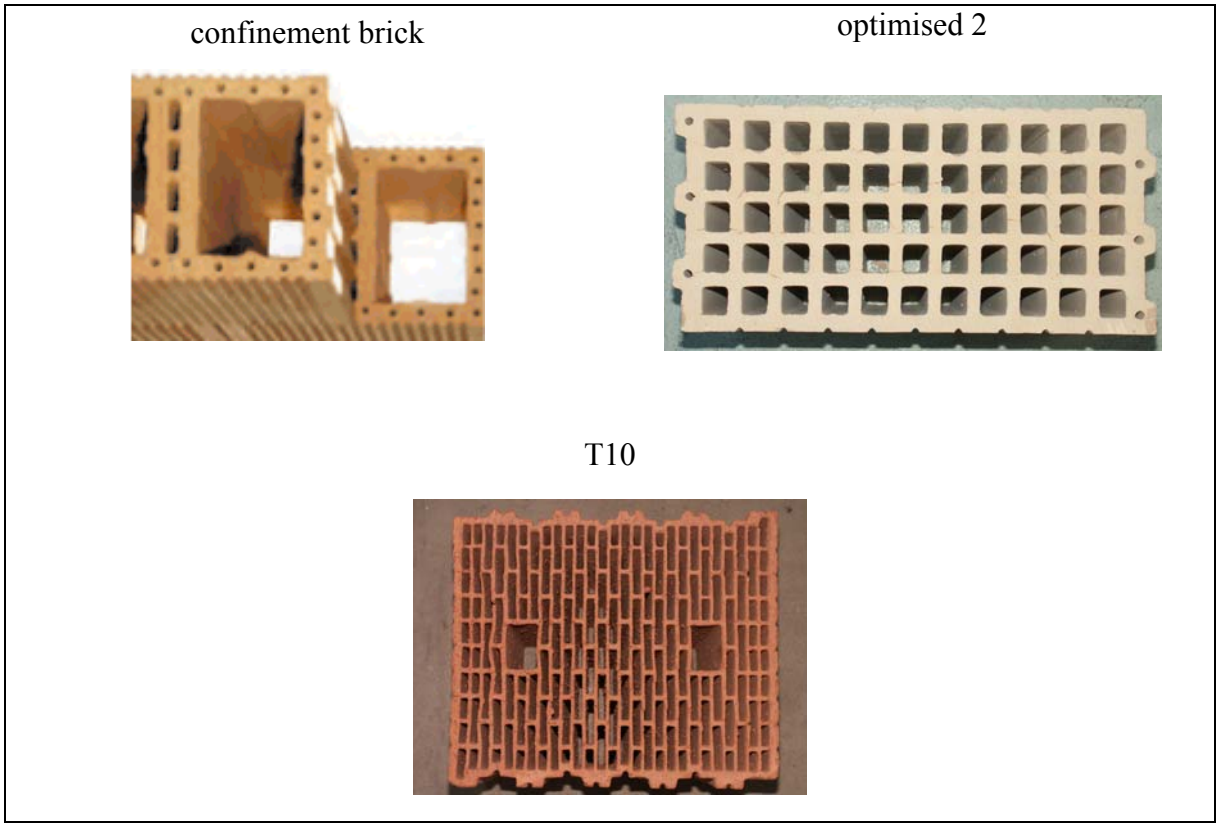

figure 1: different hole patterns of the clay bricks

2.1.2. Mortar

- General purpose mortar
  ready-mixed mortar M5 according to DIN EN 998-2
- Thin layer mortar
  Bellenberger Planziegel thin layer mortar
  Generally approved by the building authorities (DIBT Zul.-Nr. Z.17.1-261)
- Thin layer mortar
  Wienerberger Poroton thin layer mortar for bricks T10
  Generally approved by the building authorities (DIBT Zul.-Nr. Z.17.1-261)

2.2. Walls made of calcium silicate units

2.2.1. Units

Optimised calcium silicate bricks (see [6]) were used for the pseudo dynamic tests. Each of them had a width of 175 mm, a length of 249 mm and a height 248 mm.

2.2.2. Mortar

- Thin layer mortar
  Mortar class M10 according to DIN EN 998-2

3. Pseudodynamic test

3.1. Fundamentals

The pseudo dynamic wall tests, which have a single horizontal dynamic degree of freedom (DOF) shall be comparable with the tests performed at JRC [1] with two horizontal degrees of freedom. Thus, equation (1) had been deduced to consider the effect of two floors on the test specimen with only a single degree of freedom.

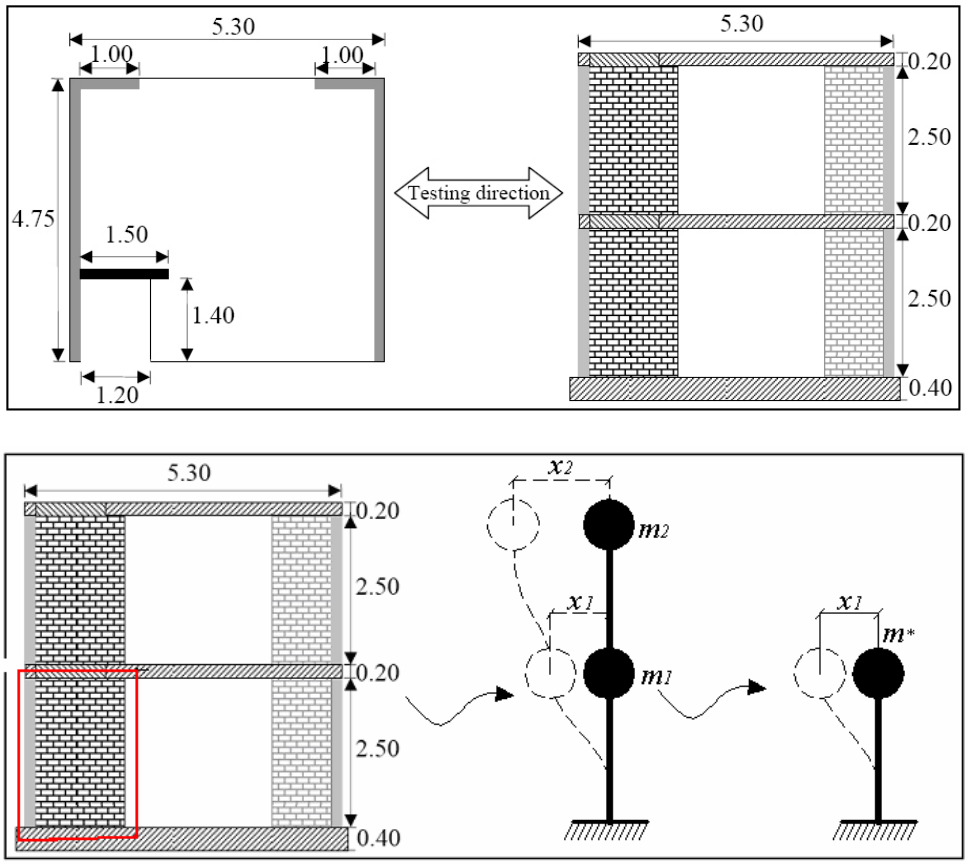

figure 2: ground plan and view of the Ispra specimen [1]

$$\left.\begin{aligned} m_1 \cdot \ddot{x}_1 + k_1 \cdot x_1 - k_2 \cdot (x_2 - x_1) &= -m_1 \cdot \ddot{x}_g \\ m_2 \cdot \ddot{x}_2 + k_2 \cdot (x_2 - x_1) &= -m_2 \cdot \ddot{x}_g \end{aligned}\right\} \Rightarrow m^* \cdot \ddot{x}_1 + k_1 \cdot x_1 = -m^* \cdot \kappa \cdot \ddot{x}_g \qquad (1)$$

Equation (1) considering the nonlinear behaviour of the wall and the damping can be written as follows:

$$m^* \cdot \ddot{x}(t)_1 + c \cdot \dot{x}(t)_1 + f_1(t) = -m^* \cdot \kappa \cdot \ddot{x}(t)_g \qquad (2)$$

with

$$m = m_1 + \frac{1}{\Psi} \cdot m_2 \qquad (3)$$

Considering only the inner transverse wall in the test, only a fraction of the total story masses has to be taken into account. This has been estimated by the ration of the bending stiffness of the wall under consideration to the overall bending stiffness of the walls in the pertinent direction.

$$m^* = \iota \cdot m \qquad (4)$$

$$\iota = \frac{I_{wall}}{\Sigma I} \qquad (5)$$

$$\psi = \frac{x_1}{x_2} \qquad (6)$$

$$\kappa = \frac{\sum m}{m^*} = \frac{m_1 + m_2}{m_1 + \frac{1}{\Psi} \cdot m_2} \qquad (7)$$

I_{wall} stiffness of the regarded wall

ΣI stiffness of all walls arranged in the ground plan of the building.

$f_1(t)$ reaction of the wall in the direction of ground acceleration.

3.2. Pseudo dynamic algorithm

The implicit $\alpha-$Method has been used for solution of motion equation (2) according to [12].

After input the excitation $\ddot{x}(t)_g$ and initialisation of all variables the procedure begins to perform the following operation at each time step $dt_{(i)}$:

a) Substituting the values of all variables, which have been calculated in the last time step dt_{i-1}, in the motion of equation and for $dt_{(i)}$.

b) Calculate the error of the displacements $\Delta d_{(i,n)}$ in solving the equation of motion and checking if the error is smaller than the admissible tolerance.

c) When the error of the displacements is smaller than the tolerance, then the response of the structure at the time step $dt_{(i)}$ is $d_{(i)} = dex_{(i)} + \Delta d_{(i,n)}$. In this case, the procedure saves the results (response and reaction of structure) in a txt-file and starts to perform the next time step $dt_{(i+1)}$, else the procedure begins the implicit iteration in time step $dt_{(i)}$ (Ramp Period).

d) Applying the displacements dc on the test structure step by step and measure the deformation of the wall $dex_{(i,n)}$ and reaction $rex_{(i,n)}$ in the direction of the ground acceleration.

e) Exchanging the new measurement values in equation of motion and repeating the steps b,c,d, and e until the condition in step c fulfilled. Figure 3 shows the arrangement of performed operations in the procedure.

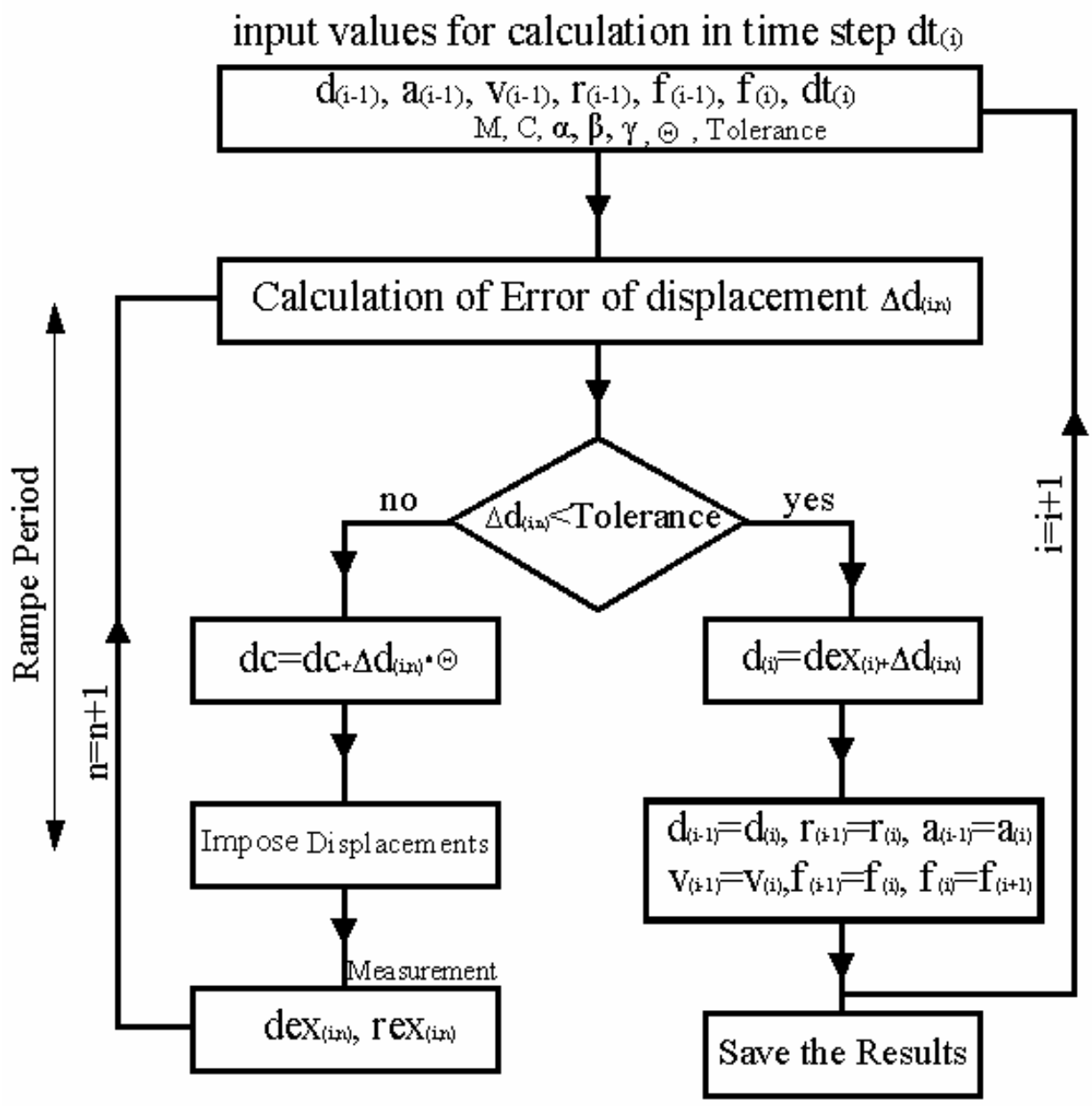

Figure 3: Performed Operations in Procedure

The last four steps are repeated for every iteration step within time step dt_i. Each iteration step can be subdivided into two phases, the "hold period" and the "ramp period", see figure 4. During the ramp period, the target displacement is applied in an iterative procedure.

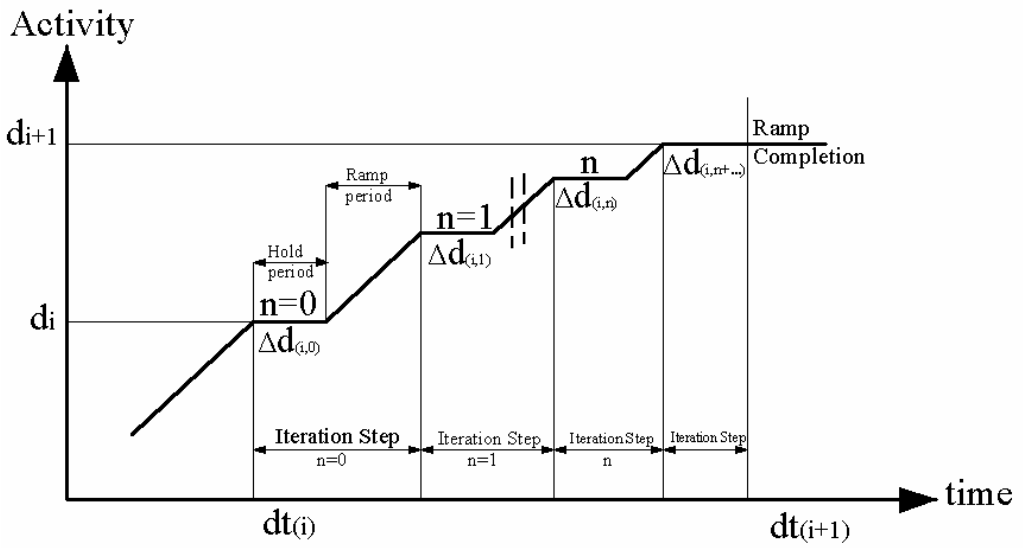

figure 4: Tasks performed in each step of a pseudodynamic test

In each iteration step the error, which has been calculated in step b in solving the equation of motion is used for improving the imposed displacement, so that the convergence of solution accelerates quickly, see figure 5.

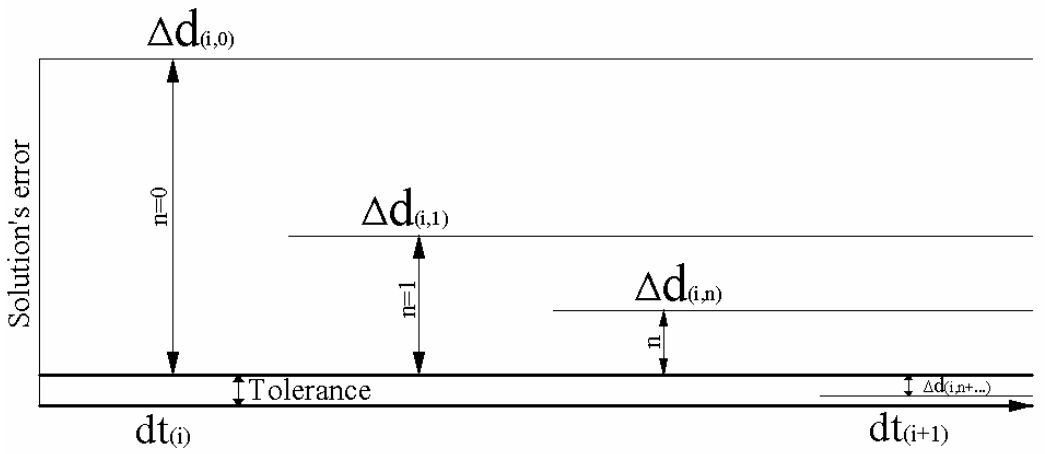

figure 5: convergence diagram of solution of motion equation

3.3. Mass data for the wall tests

The basis for the pseudo dynamic wall tests are the tests carried out at JRC (see [1]). Based on the masses of the specimens at JRC, the masses for the wall tests were calculated. Table 1 shows the masses of the structural elements of the JRC specimens.

table 1: overview of the mass of the structural elements

structural element	mass
slab	12.4 to per story
additional mass	5.2 to per story
roof structure	2.9 to
floor KS (walls)	11.4 to per story
floor clay (walls)	4.9 to per story

In the calculations (8) to (11) the floor masses (floor 1 and floor 2) for the specimen made of calcium silicate bricks and the specimen made of clay bricks are calculated.

$$m_{KS,1} = 12.4 + 5.2 + 11.4 = 29.0 \text{ to} \quad (8)$$

$$m_{KS,2} = 12.4 + 5.2 + 2.9 + 11.4/2 = 26.2 \text{ to} \quad (9)$$

$$m_{clay,1} = 12.4 + 5.2 + 4.9 = 22.5 \text{ to} \quad (10)$$

$$m_{clay,2} = 12.4 + 5.2 + 2.9 + 4.9/2 = 23.0 \text{ to} \quad (11)$$

3.4. Test programme

Eight pseudo dynamic wall tests were performed at Kassel University. Six were based on clay bricks with a width of 175 mm and 300 mm and two on calcium silicate units with a width of 175 mm (see table 2). All of these walls were tested with a support simulating a restraint of rotation at the top of the wall, so that the point of zero moment is at mid height of the wall as described in [4] and [5].

table 2: overview of the wall tests

No.	specimen	kind of brick	length of the wall [m]	vertical stress [N/mm²]	ψ [-]	κ [-]	ι [-]	m [to]	Stiffness
1	PSD-HLZ-opti2-220-190-1	Clay opti2	2.20	0.50	0.35	0.51	1.0*	89,6*	50.000
2	PSD-HLZ-opti2-220-95-1	Clay opti2	2.20	0.25	0.35	0.51	1.0*	89,6*	20.000
3	PSD-KS-opti-250-150-1	KS opti	2.50	0,34	0.35	0.53	0.87	90.4	10.000
4	PSD-KS-opti-150-90-1	KS opti	1.50	0,34	0.35	0.53	0.62	64.4	50.000
5	PSD-HLZ-opti2-110-95-1	Clay opti2	1.10	0,50	0.35	0.51	0.37	32.8	20.000
6	PSD-FZ-150-90-1	confined	1.50	0,34	0.35	0.51	0.62	55.6	50.000
7	PSD-HLZ-opti2-150-90-1	Clay opti2	1.50	0,34	0.35	0.51	0.62	55.6	25.000
8	PSD-T10-100-60-1	T10	1.00	0,20	0.35	0.51	0.21	18.8	15.000

*to play it safe (calculational 0.82)

3.5. Test procedure

For each test the acceleration input (same as for the pseudo dynamic JRC-tests and the shaking table tests), shown in figure 6, was used. Figure 7 shows the response spectra for this time history. Each test has been performed for multiple times with different values of the maximum acceleration. Normally four tests were carried out for each specimen with a duration of the test of about one hour. The time history for each test are shown in Annex A.

The test has to be stopped, if either

- the normal forces cannot be taken anymore by the specimen,
- the expected damage for the next scaling step would be excessive

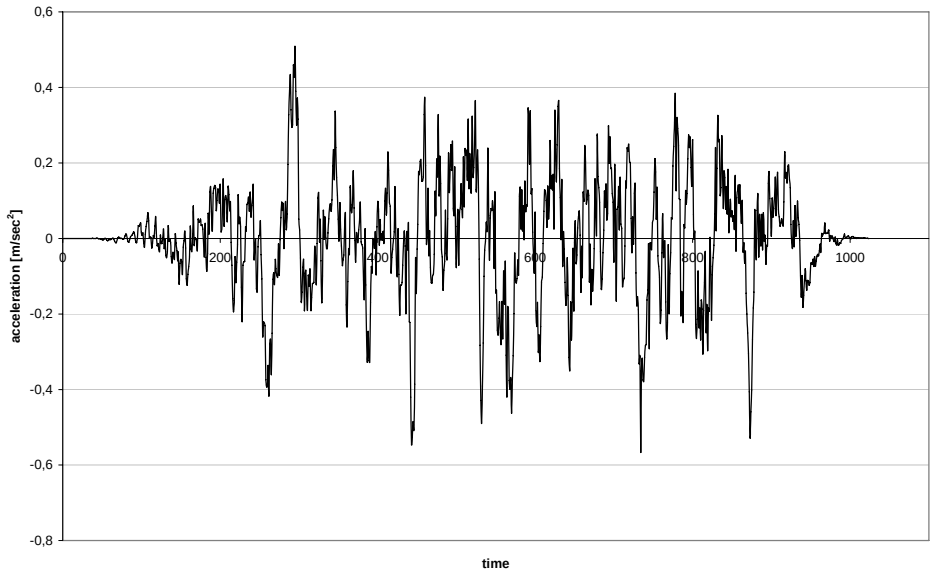

figure 6: time history generated to match elastic response spectrum type 1

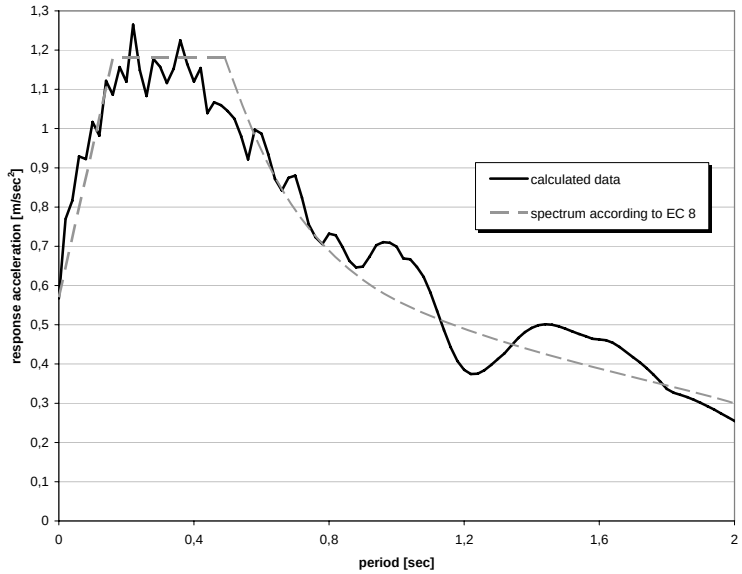

figure 7: response spectrum

In the following the distinctive features of each test are described. The horizontal force is under compression (negative value) when the hydraulic jack is moving from the left to the right hand side and under tension (positive value) when moving the other way around.

3.5.1. Test No. 1

At a horizontal force of about +65 kN cracking was audible. At a horizontal force of about -85 kN first cracks (see figure A1-1) were visible in the bottom right corner of the wall. During the course further cracks occurred and a gaping of the head joints was visible (see figure A1-2).

3.5.2. Test No. 2

At a horizontal force of about -50 kN cracking was audible. At a horizontal force of about -57 kN first cracks (see figure A2-1) were visible in the upper left corner of the wall. During the course a gaping of the head joints and the bed joints on the diagonal from the upper left corner to the bottom right corner was visible (see figure A2-2).

3.5.3. Test No. 3

At a horizontal force of about -75 kN first cracks (see figure A3-1) were visible in the upper left corner of the wall. During the course a gaping of the head joints and the bed joints on the diagonal from the upper left corner to the bottom right corner was visible (see figure A3-2).

3.5.4. Test No. 4

At a horizontal force of about +35 kN first cracks in the joints (see figure A4-1) were visible in the bottom right corner of the wall. After the test with a maximum acceleration of 0.12·g a failure in the operation system led to a horizontal deformation of the wall of about 30 mm. The crack pattern of the wall after the test with a maximum acceleration of 0.16·g is shown in figure A4-2.

3.5.5. Test No. 5

At a horizontal force of about -38 kN first vertical cracks (see figure A5-1) were visible. During the course a gaping of the bed joints on the bottom beam and under the top beam occurred.

3.5.6. Test No. 6

At a horizontal force of about +60 kN first cracks were visible in the upper right corner of the wall. During the course a gaping of the bead joints on the bottom beam and under the top beam accrued. (see figure A6-1 and A6-2).

3.5.7. Test No. 7

At a horizontal force of about -50 kN cracking was audible and visible on the diagonal from the upper left corner to the bottom right corner (see figure A7-1). The wall failed suddenly by a local crash of the corner block (see figure A7-2).

3.5.8. Test No. 8

At a horizontal force of about +31 kN cracking was audible. During the course a gaping of the bead joints on the bottom beam and under the top beam accrued. (see figure A8-1). The first crack was visible at the maximum horizontal force (see figure A8-2).

4. Test results

4.1. Comparison of the maximum horizontal force

To compare the load bearing capacity of the walls (all tested with a restraint due to the floor slabs) the non dimensional values l' and τ' have to be adopted (as available in deliverable 7.1a [5]).

$$l' = \alpha \cdot l_w / h_w \tag{12}$$

$$\alpha = \frac{\sigma_v}{f_k} \tag{13}$$

$$\tau' = \frac{H_F}{f_k \cdot A_w} \tag{14}$$

with: σ_v = normal stress due to vertical loading of the wall
f_k = compressive strength of masonry
l_w = length of the wall
h_w = height of the wall
H_F = maximum horizontal force
A_w = base area of the wall

Figure 8 displays τ' against l'. For the two walls built of calcium silicate units it could be determined, that the compressive strength of the mortar was rather low. The mortar strength was only about 7 % lower than the minimum requirement according to the code, but about 50% lower than reference values of the static cyclic tests. So, on the one hand the low strength of the mortar might be a reason for the rather low load bearing capacity of these two walls. On the other hand the higher f_k of the calcium silicate unites (in comparison to the clay brick walls) leads to a lower non dimensional shear bearing capacity τ'.

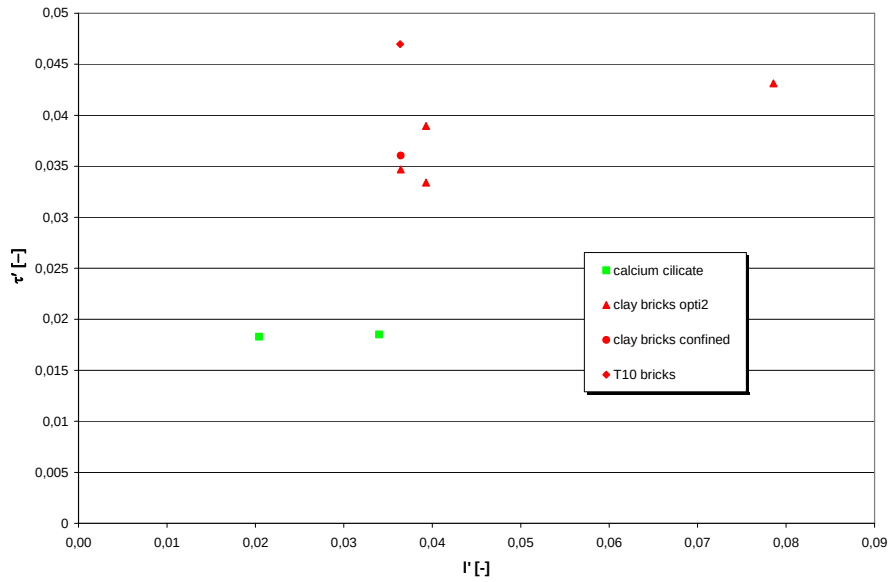

figure 8: comparison of the non dimensional load bearing capacity

4.2. Comparison of static cyclic with pseudo dynamic wall tests

Figure 9 to figure 11 show the comparison of the pseudo dynamic wall tests with static cyclic wall tests of [5]. In general, the same types of units and mortar have been used for the specimens of each comparison. However, for the comparison presented in figure 9 it has to be noted, that general purpose mortar had been used in the static-cyclic test instead of thin layer mortar.

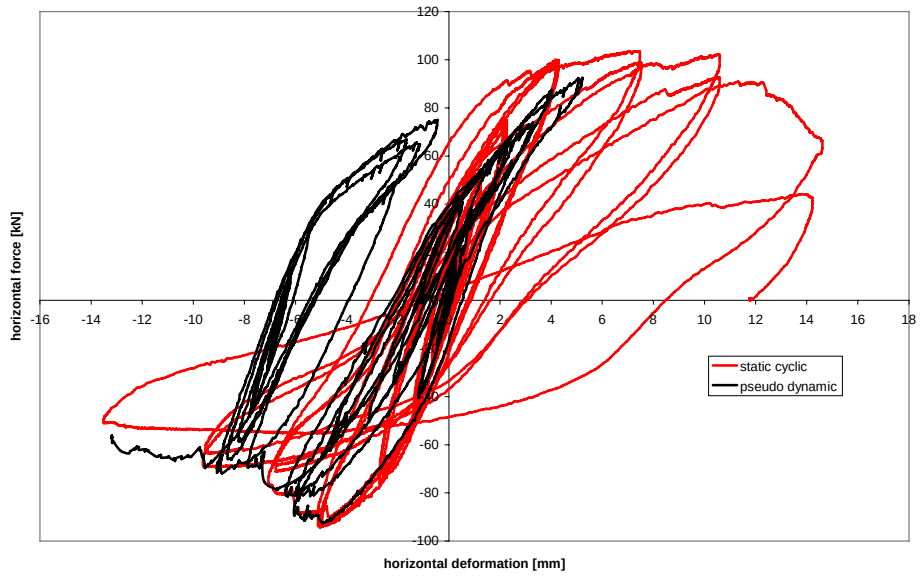

figure 9: comparison of the hysteresis of wall No. 1 with the static cyclic reference test

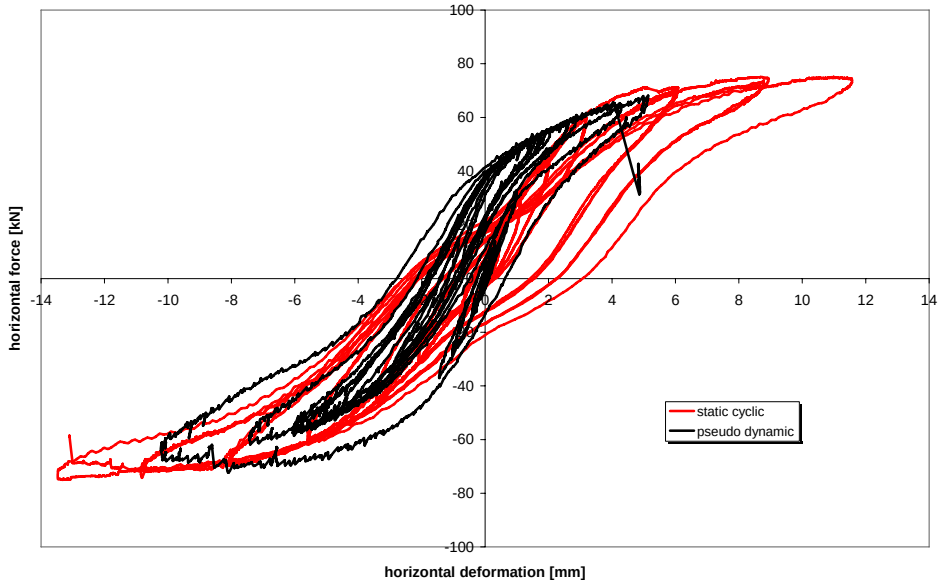

figure 10: comparison of the hysteresis of wall No. 2 with the static cyclic reference test

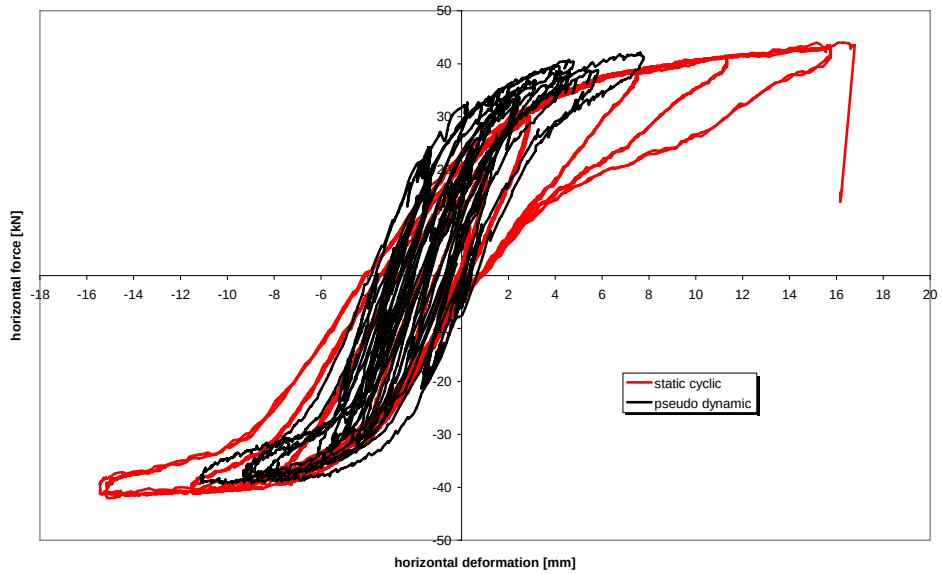

figure 11: comparison of the hysteresis of wall No. 5 with the static cyclic reference test

The hysteresis curves obtained by the pseudo dynamic test procedure show nearly the same behaviour than the curves obtained by the static cyclic test procedure. The load bearing capacity of the specimens under static cyclic loading is in average for each comparison 5% higher than for the pseudo dynamic test procedure. The deformation capacity seems to be higher under static cyclic loading, too. This result, however, may be explained by the different criteria for the end of the testing for static-cyclic versus pseudo dynamic experiments.

4.3. Deformation capacity of the walls

In table 3 an overview of the deformation behaviour of all tested walls is given. The results are interpreted according to deliverable D7.1a [5], but only test runs, which ran through the full time history were evaluated. The enveloping curves of the tests with the highest maximum acceleration, which ran a full time history are given in annex A. All values in these tables are given with the indices 1 and 2. The values with index 1 correspond to the curve segment in the third quadrant, the index 2 corresponds to the first quadrant.

table 3: overview of the deformation behaviour of clay bricks

No.	name	d_{u1} [mm]	d_{u2} [mm]	d_{cr1} [mm]	d_{cr2} [mm]	H_{cr1} [kN]	H_{cr2} [kN]	K_{e1} [N/m]	K_{e2} [N/m]	Hu1	Hu2	d_{e1} [mm]	d_{e2} [mm]	μ_1 [-]	μ_2 [-]
1	PSD-HLZ-opti2-220-190-1	5.2	4.7	2.1	1.7	69	67	33	39	90	92	2.7	2.3	1.9	2.0
2	PSD-HLZ-opti2-220-95-1	7.0	4.3	2.5	1.7	46	46	18	27	63	61	3.4	2.3	2.0	1.9
3	PSD-KS-opti-250-150-1	17.0	9.4	1.9	2.0	58	56	31	28	83	80	2.7	2.9	6.3	3.3
4	PSD-KS-opti-150-90-1	8.6	6.5	2.2	2.0	33	28	15	14	44	38	2.9	2.7	2.9	2.4
5	PSD-HLZ-opti2-110-95-1	11.1	7.7	2.3	1.6	27	29	12	18	36	39	3.1	2.2	3.6	3.6
6	PSD-FZ-150-90-1	9.7	5.2	2.7	1.8	36	41	13	23	50	58	3.8	2.5	2.6	2.0
7	PSD-HLZ-opti2-150-90-1	5.3	5.0	1.4	1.7	36	36	26	21	50	48	1.9	2.3	2.7	2.2
8	PSD-T10-100-60-1	12.3	7.5	2.8	1.7	18	22	6	13	24	30	3.7	2.3	3.3	3.2

To compare the ductility of the walls the average ductility is given by equation (15).

$$\mu' = \frac{\mu_1 + \mu_2}{2} \tag{15}$$

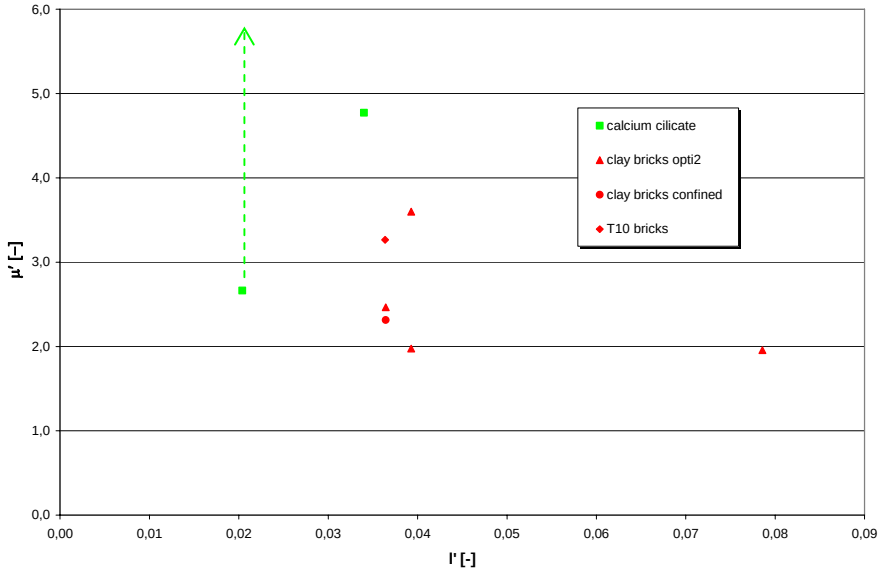

figure 12: comparison of the ductility

Figure 12 compares the ductility of all tested walls with clamping due to the floor slabs. The ductility calculated by equation (15) is shown against the value l' according to equation (12). An enhancement of the ductility by decreasing l' is expected, but cannot be verified by all tests. This is because of the different abort criterion for each test and because the comparison corresponds only to those tests, which run through the full time history.

The measured ductility for the calcium silicate wall with the lowest value of l' is rather small, because the wall was damaged before the test by a failure in the operation system. So it was not possible to test the wall with higher horizontal deformations, but it can be assumed that this might have been possible without damaging the wall before the test.

Finally it has to be minded, that all tested walls had a rather low vertical loading. Hence, it is not possible to transfer these results directly to walls with a higher level of vertical loading.

5. Conclusions and outlook

Eight pseudo dynamic wall tests were carried out at Kassel University using the same test setup as for the static cyclic tests of deliverable D 7.1.a [5]. The walls with a height of 2.5 m shall represent one of the main walls in the ground floor of a two story terraced house as tested at JRC Ispra (see [1]). In order to approximately simulate the behavior of a masonry wall in such a building, the pseudo dynamic tests were performed as single degree of freedom tests assuming the distribution of inertia forces from the first vibration mode of the two storey building.

For each wall specimen, several test runs were performed using the same time history (artificial record reflecting a EUROCODE 8 compatible spectrum) with stepwise increasing scaling factors. For the maximum displacement achieved, the displacement ductility has been calculated according to the definition in [5].

The results show, that the maximum forces as obtained from the pseudo dynamic tests match well with the capacity determined from the pertinent static cyclic tests. For the displacement ductility, values between $\mu = 2$ and $\mu = 5$ could be found, depending on the vertical load level and the wall length. It should be noted, however, that these ductility values all have been obtained for rather low levels of vertical loading and, thus, care has to be taken to transfer these values to cases with higher exploitation of the masonry in terms of vertical loading.

In conjunction with the results from the other pseudo dynamic tests as well with the static cyclic tests, a data base for the load deformation behavior of masonry walls is now available. This enables a more realistic calculation of the capacity of masonry structures subject to lateral forces resulting from wind and seismic action.

6. Bibliography

[1] Anthoine, A.: Definition and design of the test specimen; Technical report of the collective research project ESECMaSE, deliverable D8.1, 2007

[2] Fehling, E.; Stürz, J.: Theoretical Investigation on Stress States of Masonry Structures Subjected to Static and Dynamic Shear Loads (Lateral Loads), Analysis of Terraced House; Technical report of the collective research project ESECMaSE, deliverable D3.1, 2005

[3] Fehling, E.; Stürz, J. ; Schermer, D.: Theoretical Investigation on Shear Tests Methods, Construction of test setup for shear tests for validation of proposed method; Technical report of the collective research project ESECMaSE, deliverable D6.3, 2006

[4] Fehling, E.; Stürz, J. ; Schermer, D.: Theoretical Investigation on Shear Tests Methods, Series of shear tests for validation; Technical report of the collective research project ESECMaSE, deliverable D6.4, 2006

[5] Fehling, E.; Stürz, J.; Emami, E.: Test results on the behaviour of masonry under static (monotonic and cyclic) in plane lateral loads; Technical report of the collective research project ESECMaSE, deliverable D7.1a, 2007

[6] Grabowski, S.: Tests on the relevant material properties on improved clay units; Technical report of the collective research project ESECMaSE, deliverable D2.3, 2006

[7] Graubner, C.-A.; Kranzler, T.; Schubert, P.; Simon, E.: Festigkeitseigenschaften von Mauerwerk, Teil 3: Schubfestigkeit von Mauerwerksscheiben; Mauerwerk-Kalender 2005; Ernst & Sohn; 2005

[8] Jäger, W.; Schöps, P.: Kosteneinsparung durch Ansatz realitätsnaher Bemessungskonzepte für die Schubbeanspruchung von Mauerwerksbauten; Frauenhofer IRB Verlag; 2005

[9] Ötes, A.; Löring, S.: Tastversuche zur Identifizierung des Verhaltensfaktors von Mauerwerksbauten für den Erdbebennachweis; Abschlussbericht; Universität Dortmund; Lehrstuhl für Tragkonstruktionen; 2003

[10] Schermer, D.: Verhalten von unbewehrtem Mauerwerk unter Erdbebenbeanspruchung; Dissertation; TU München, Institut für Baustoffe und Konstruktionen, Lehrstuhl für Massivbau; 2004

[11] Schermer, D.: Theoretical Investigation on Stress States of Masonry Structures Subjected to Static and Dynamic Shear Loads (Lateral Loads), Analysis of Apartment House; Technical report of the collective research project ESECMaSE, deliverable D3.2, 2005

[12] Thiele, K.: Pseudodynamische Versuche an Tragwerken mit großen Steifigkeitsänderungen und mehreren Freiheitsgraden; Dissertation; Zürich; 2000

[13] Carydis, P.: Test results on the earthquake resistance on improved masonry materials by shaking table tests; Technical report of the collective research project ESECMaSE, deliverable D7.2c, 2008

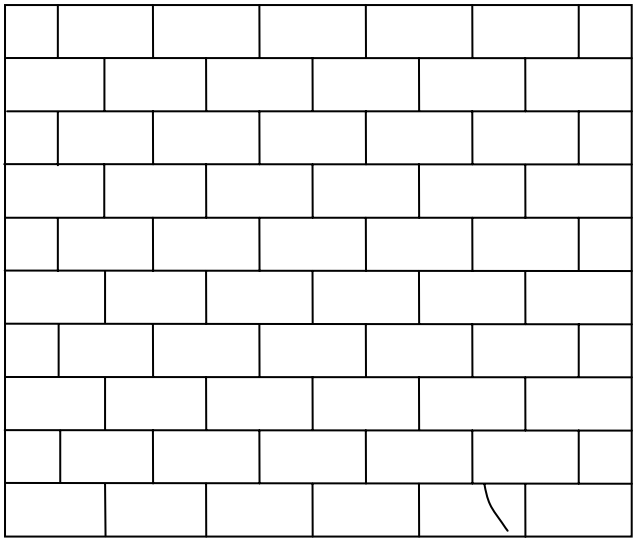

figure A1-1: first cracks at about -85 kN of wall No. 1

figure A1-2: crack pattern of wall No. 1

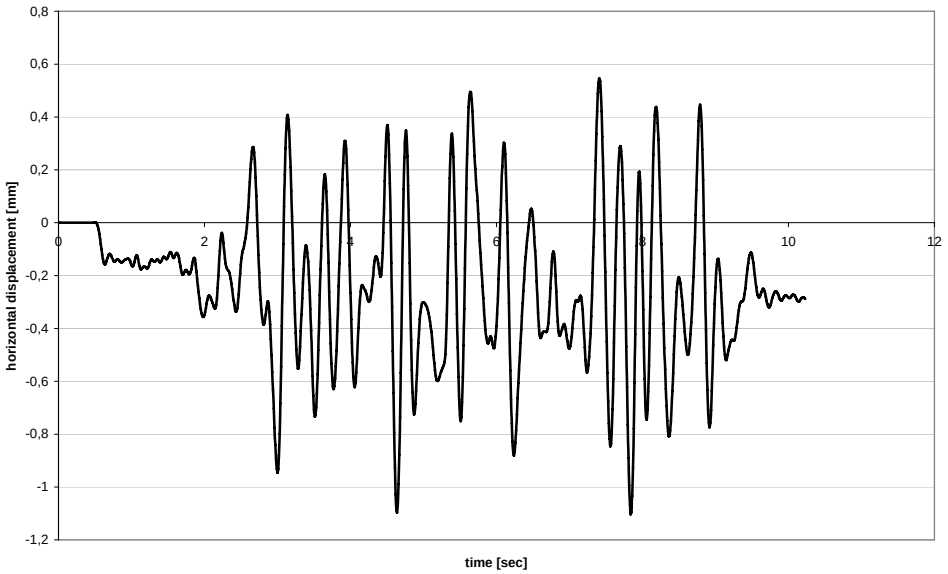

figure A1-3: time history (max. 0.08 · g) of wall No. 1

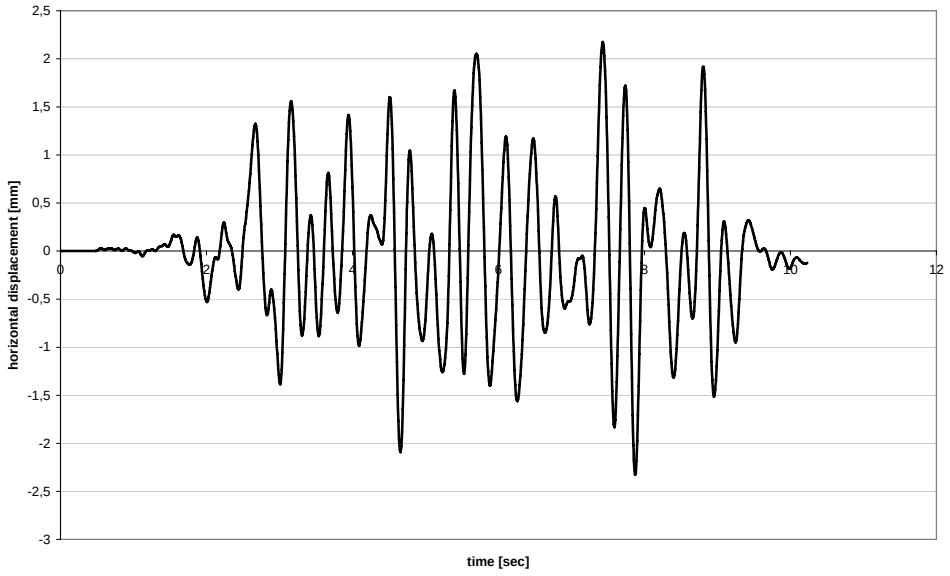

figure A1-4: time history (max. 0.16 · g) of wall No. 1

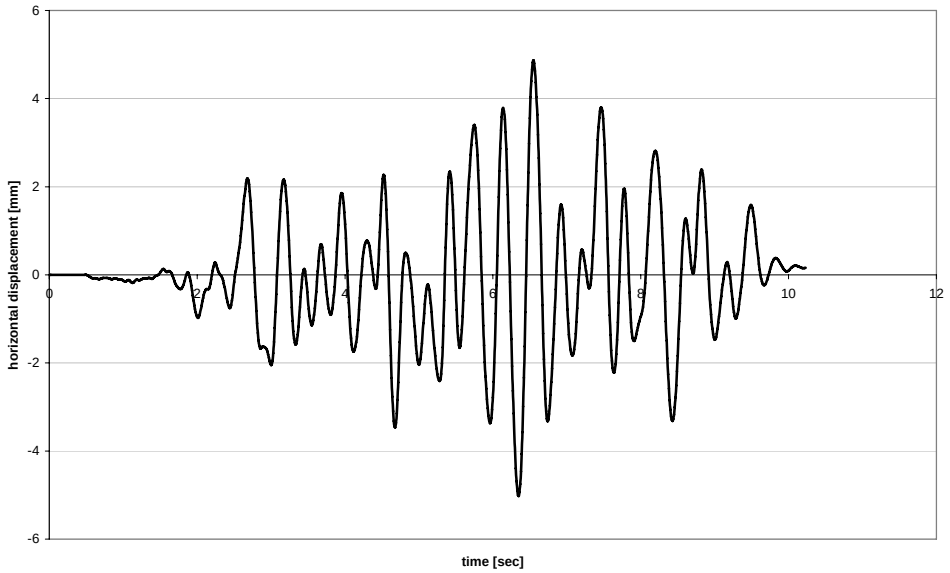

figure A1-5: time history (max. 0.23 · g) of wall No. 1

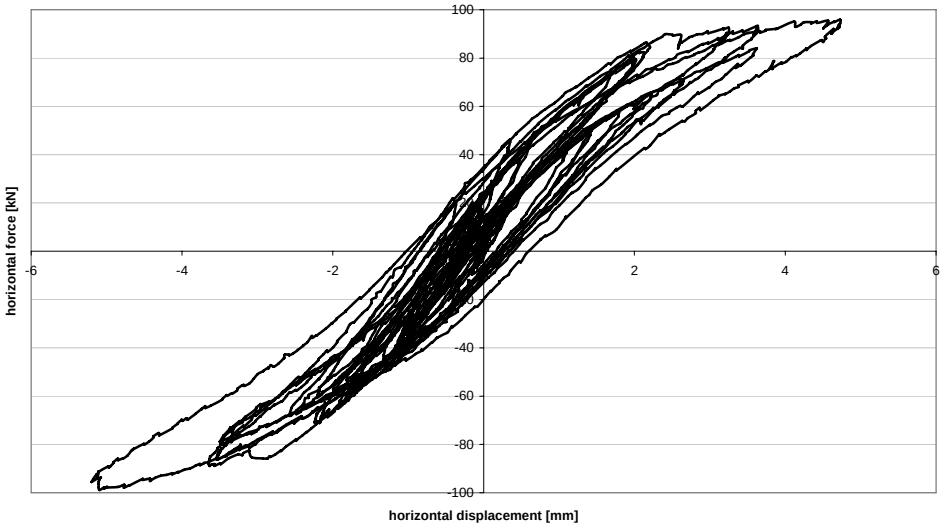

figure A1-6: hysteresis curve of wall No.1 (max. 0.23 · g)

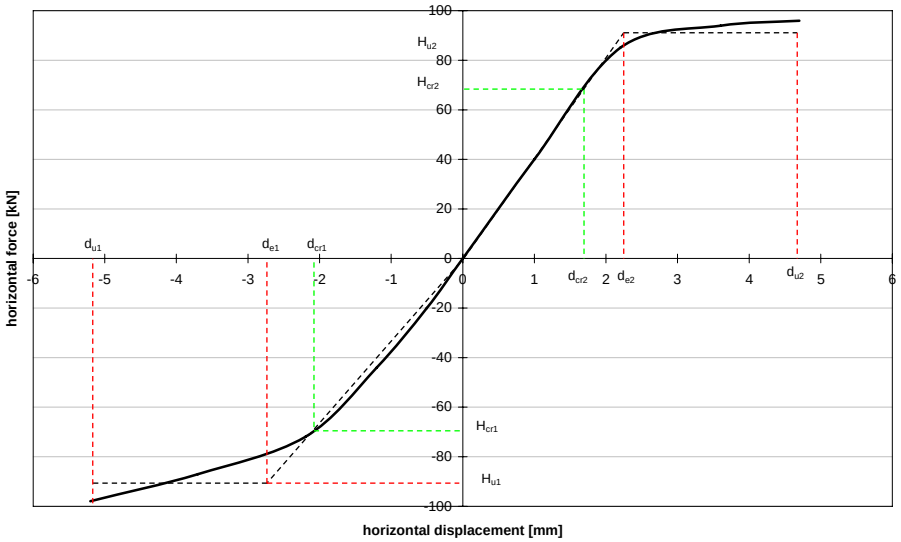

figure A1-7: enveloping curve of wall No.1 (max. 0.23 · g)

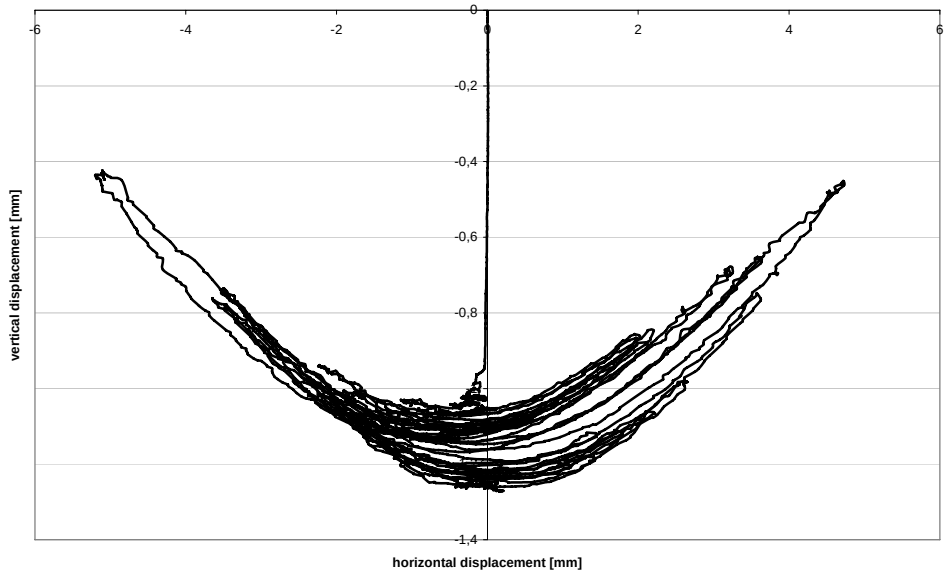

figure A1-8: vertical displacement of wall No.1 (max. 0.23 · g)

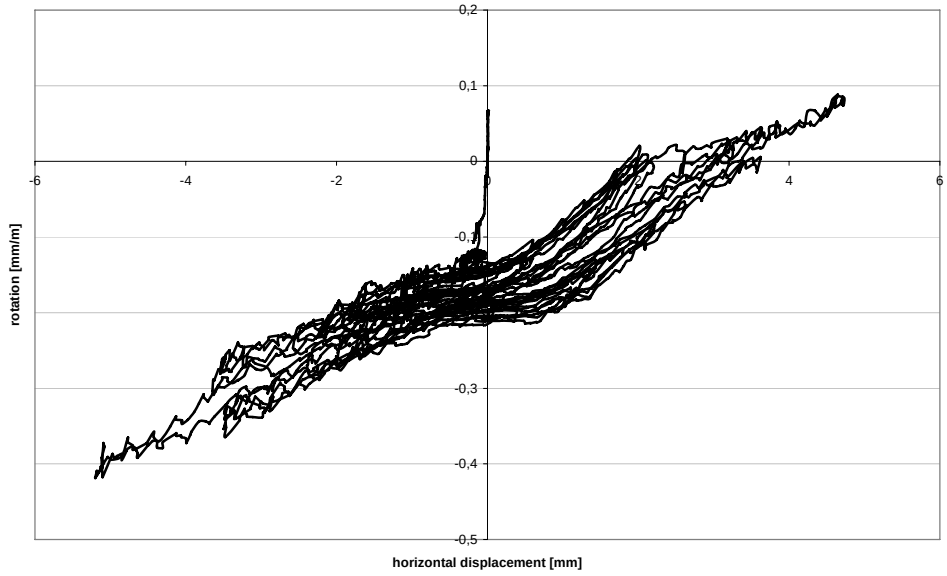

figure A1-9: rotation at the top of wall No.1 (max. 0.23 · g)

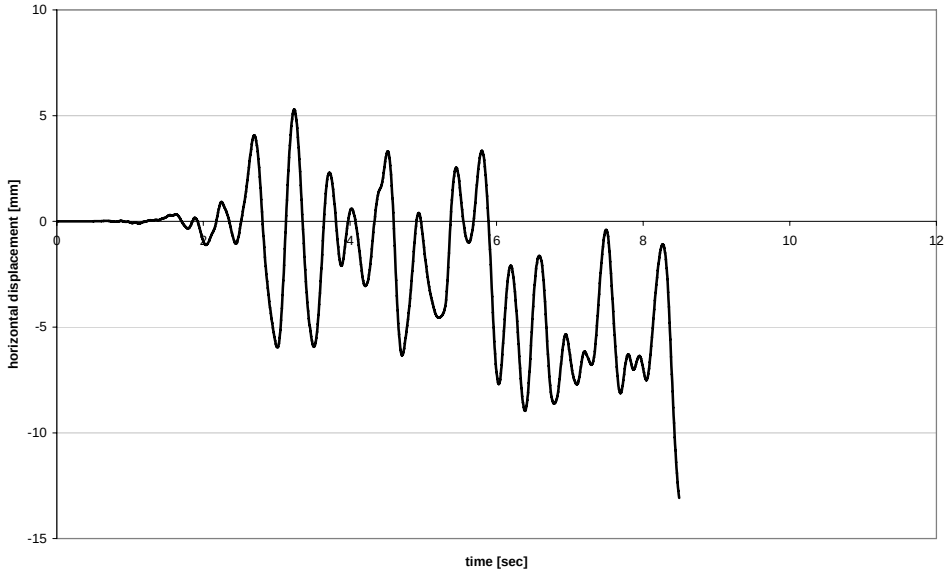

figure A1-10: time history (max. 0.25 · g) of wall No. 1 (discontinued)

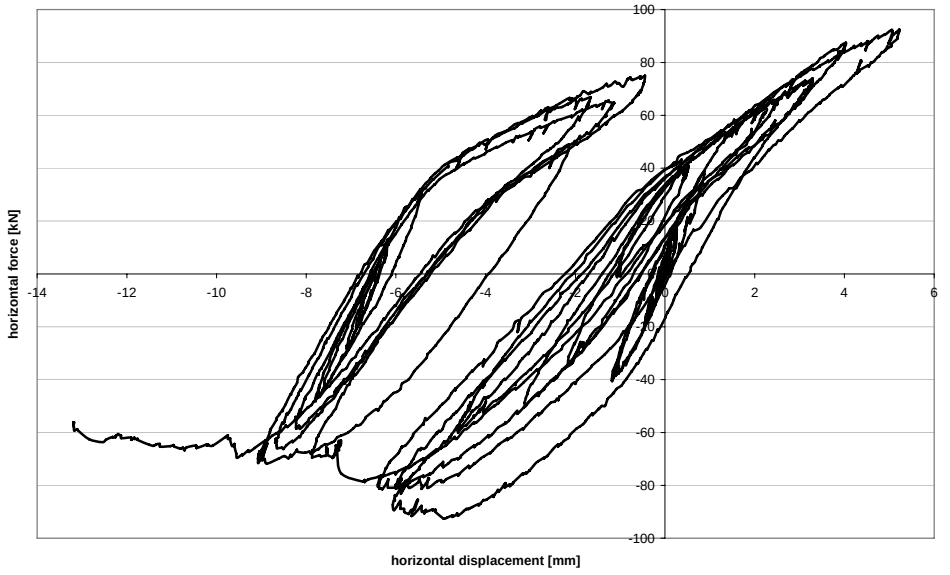

figure A1-11: hysteresis curve of wall No.1 (max. 0.25 · g)

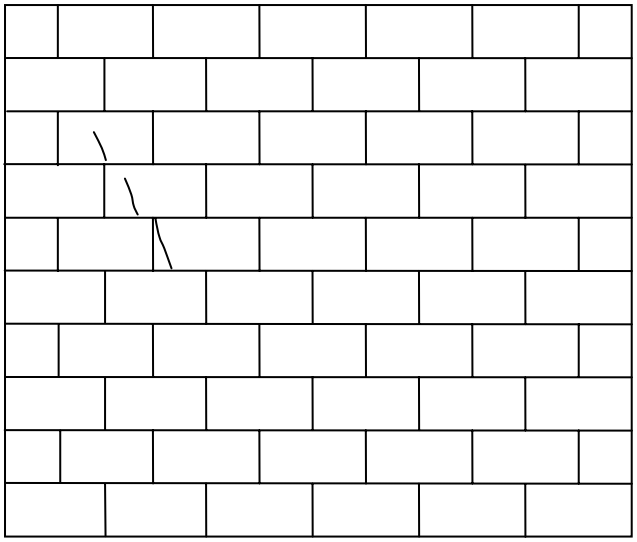

figure A2-1: first cracks at about -57 kN of wall No. 1

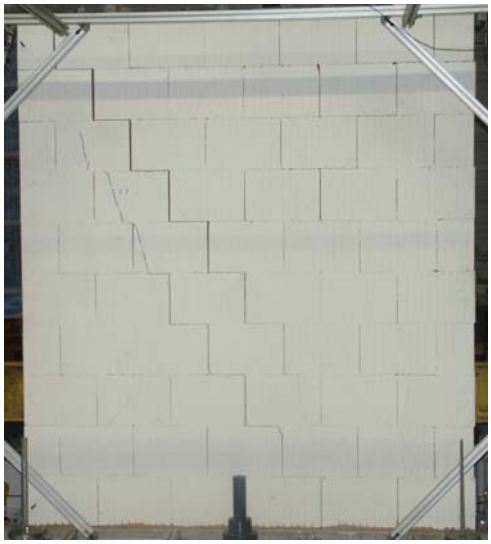

figure A2-2: crack pattern of wall No. 2

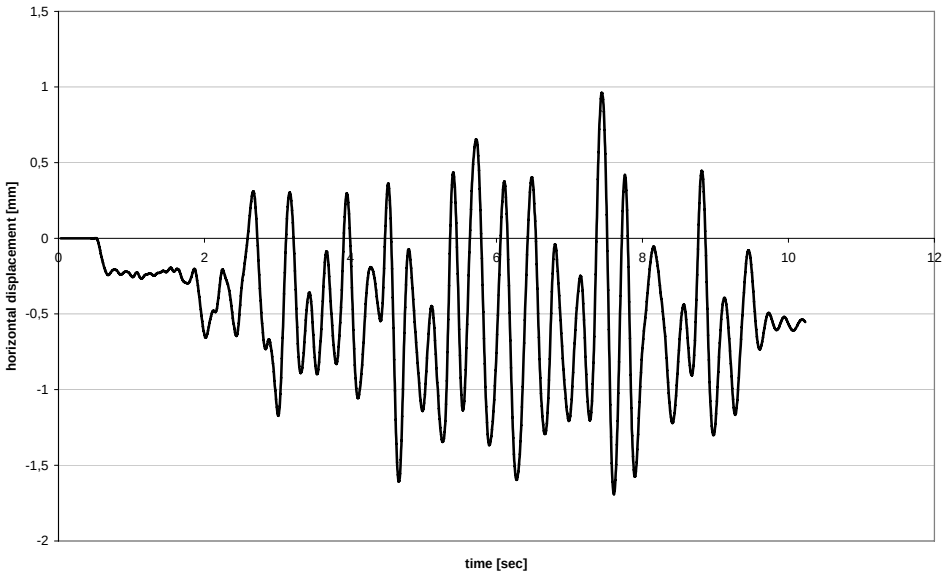

figure A2-3: time history (max. 0.08 · g) of wall No. 2

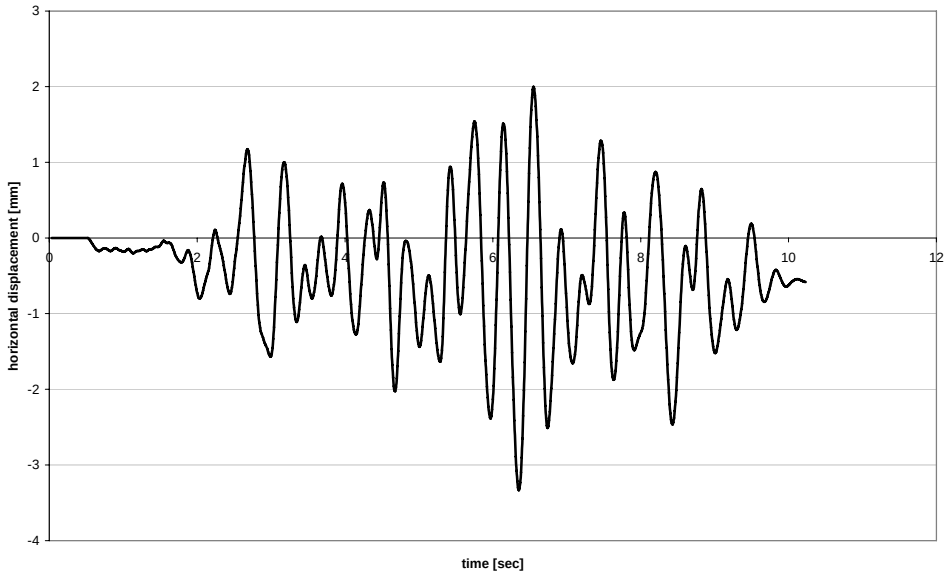

figure A2-4: time history (max. 0.12 · g) of wall No. 2

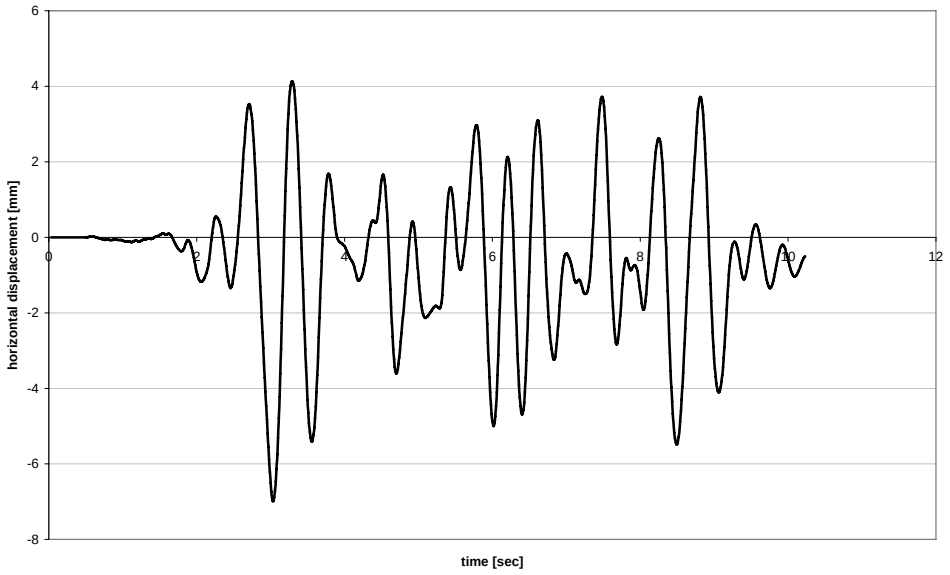

figure A2-5: time history (max. 0.18 · g) of wall No. 2

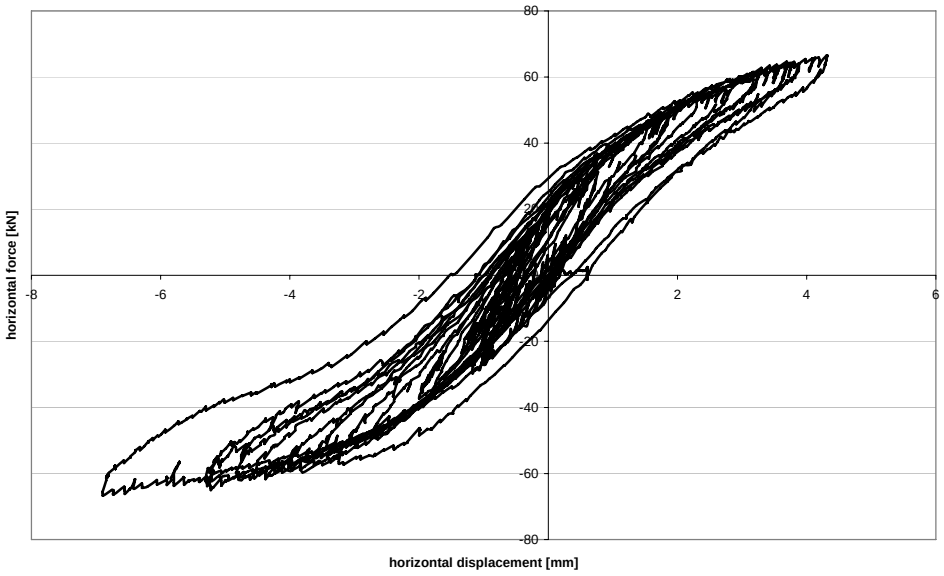

figure A2-6: hysteresis curve of wall No.2 (max. 0.18 · g)

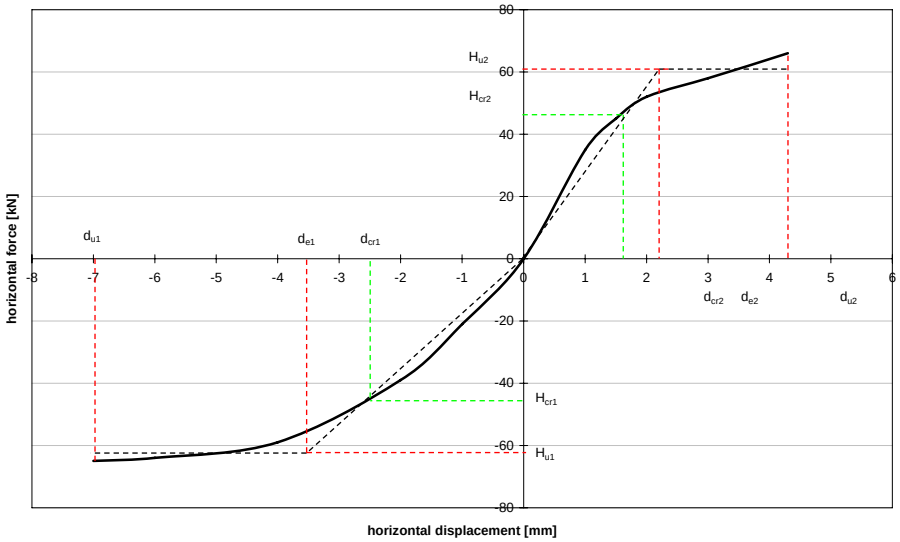

figure A2-7: enveloping curve of wall No.2 (max. 0.18 · g)

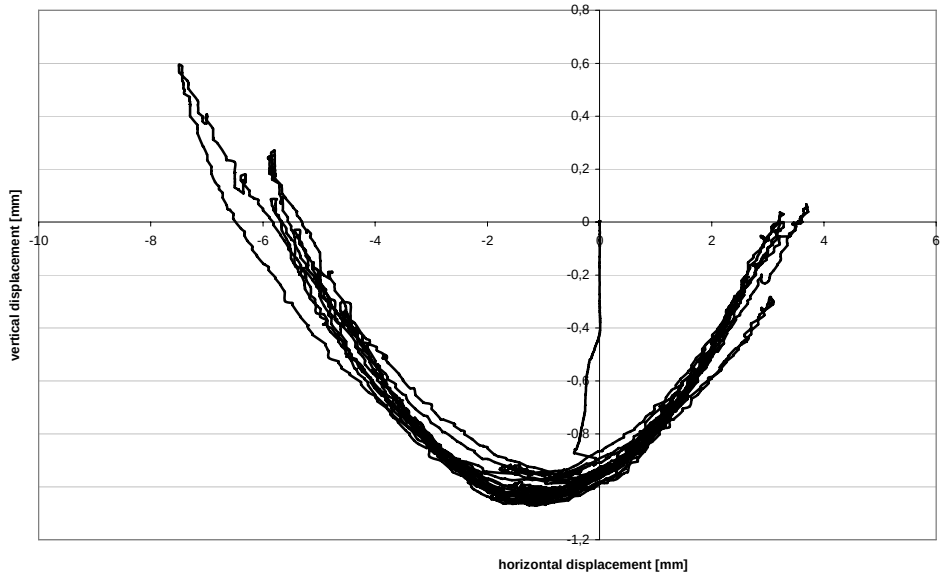

figure A2-8: vertical displacement of wall No.2 (max. 0.18 · g)

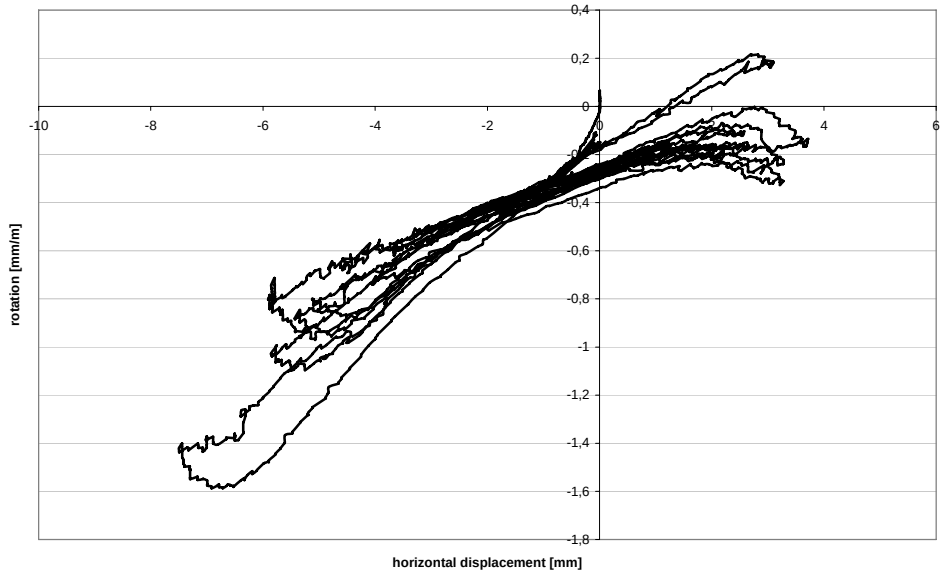

figure A2-9: rotation at the top of wall No.2 (max. 0.18 · g)

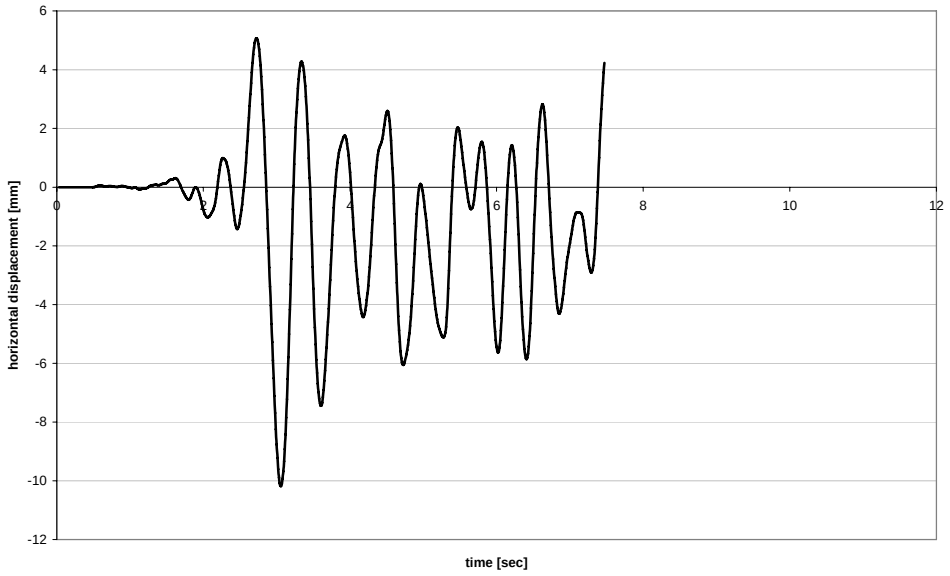

figure A2-10: time history (max. 0.20 · g) of wall No. 2

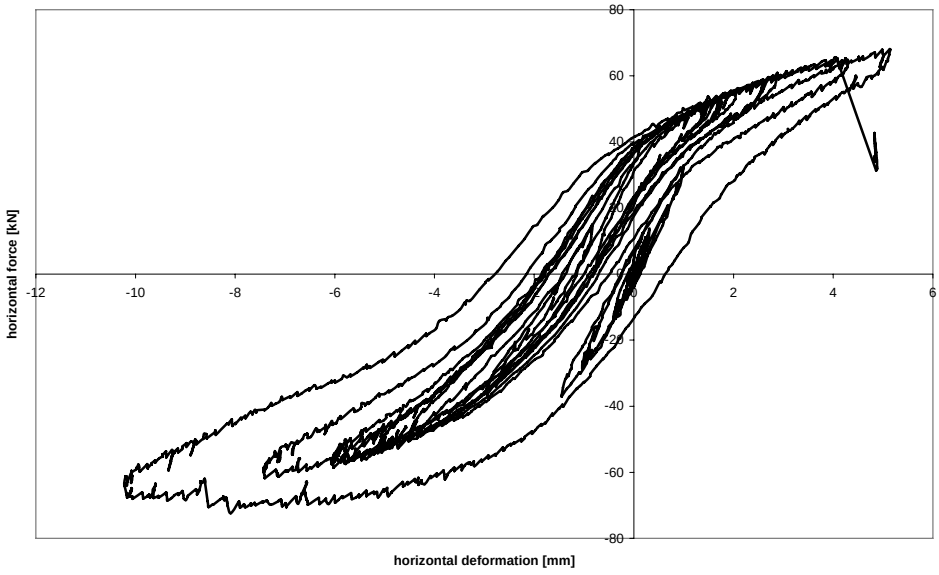

figure A2-11: hysteresis curve of wall No.2 (max. 0.20 · g)

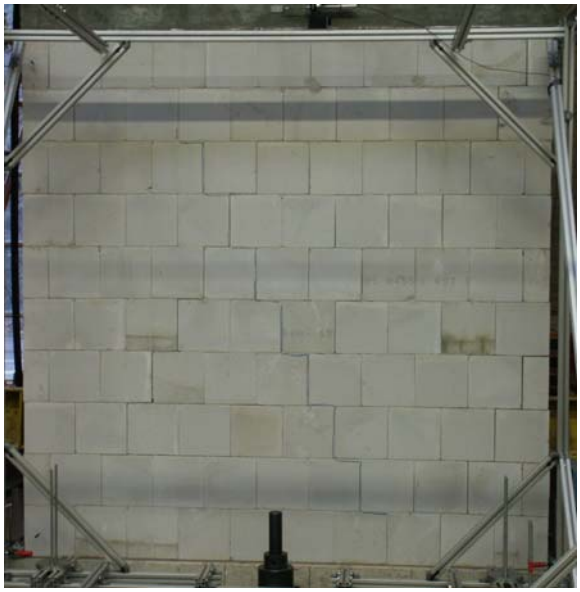

figure A3-1: first cracks at about -75 kN of wall No. 3

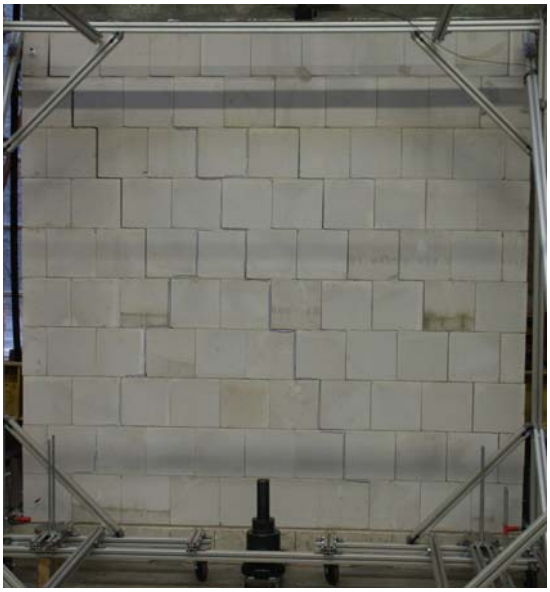

figure A3-2: crack pattern of wall No. 3

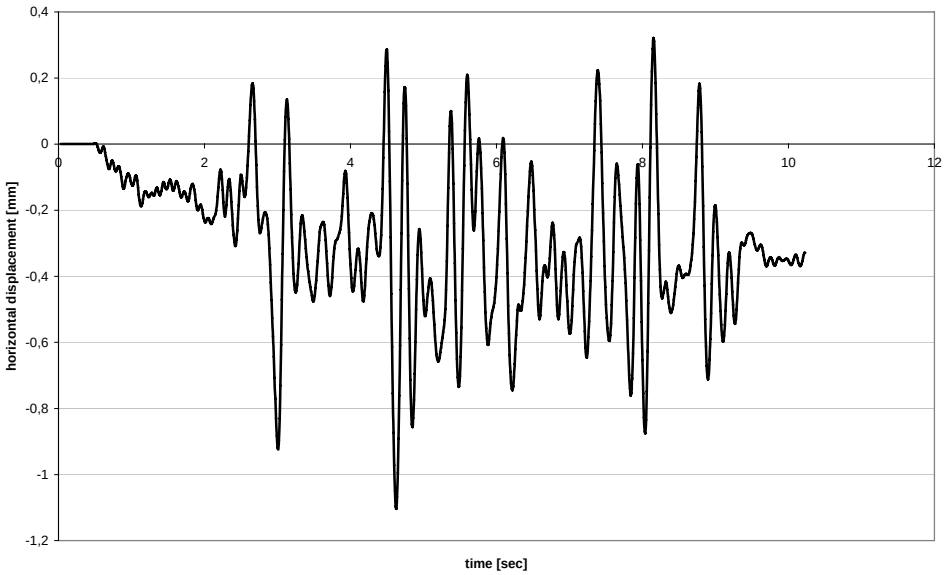

figure A3-3: time history (max. 0.08 · g) of wall No. 3

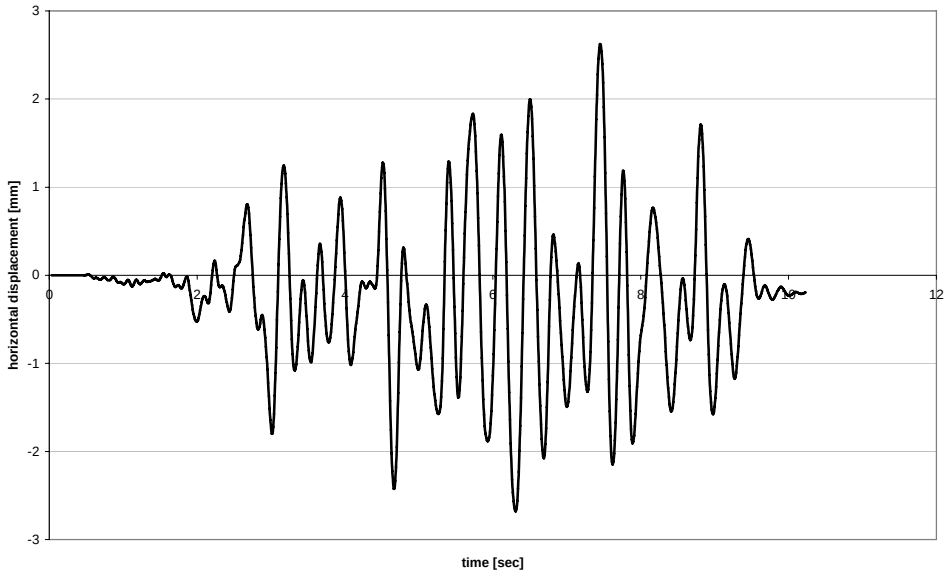

figure A3-4: time history (max. 0.16 · g) of wall No. 3

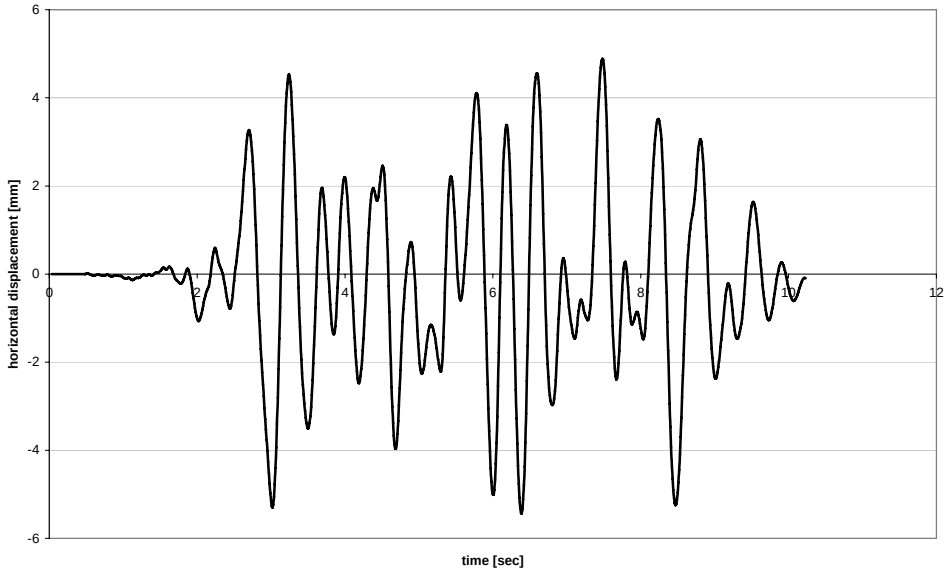

figure A3-5: time history (max. 0.24 · g) of wall No. 3

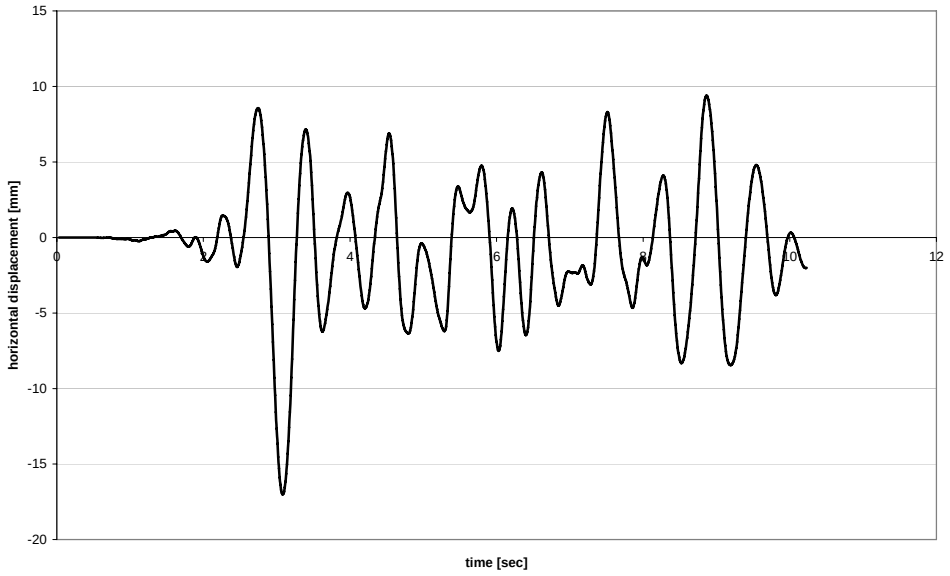

figure A3-6: time history (max. 0.32 · g) of wall No. 3

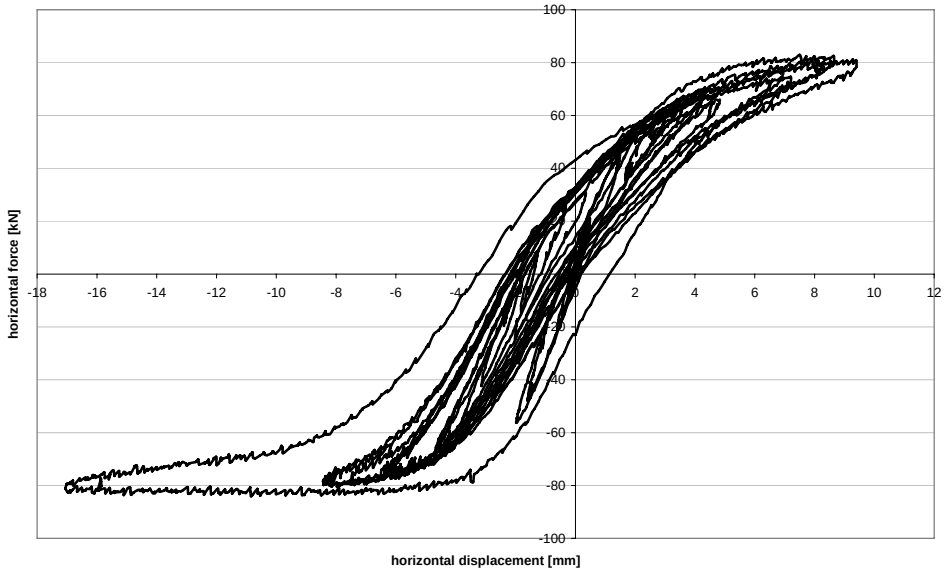

figure A3-7: hysteresis curveof wall No.3 (max. 0.32 · g)

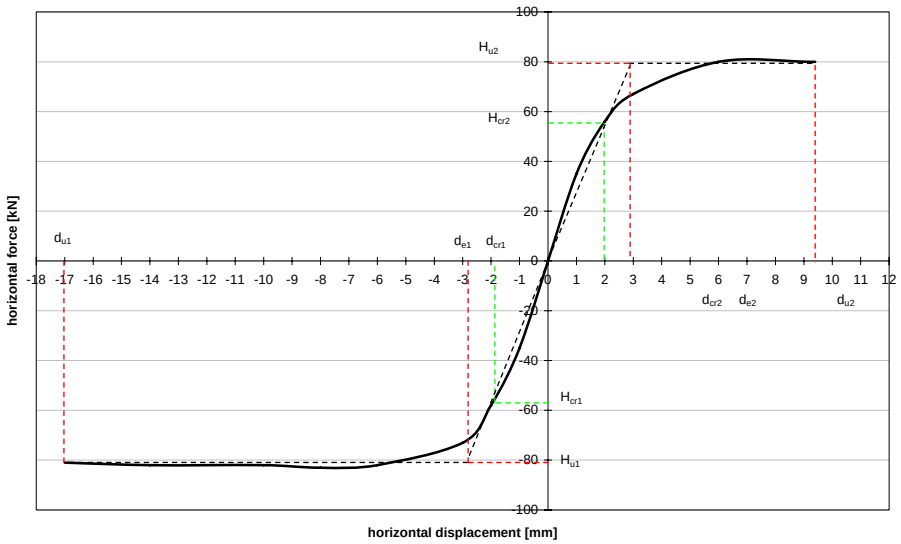

figure A3-8: enveloping curve of wall No.3 (max. 0.32 · g)

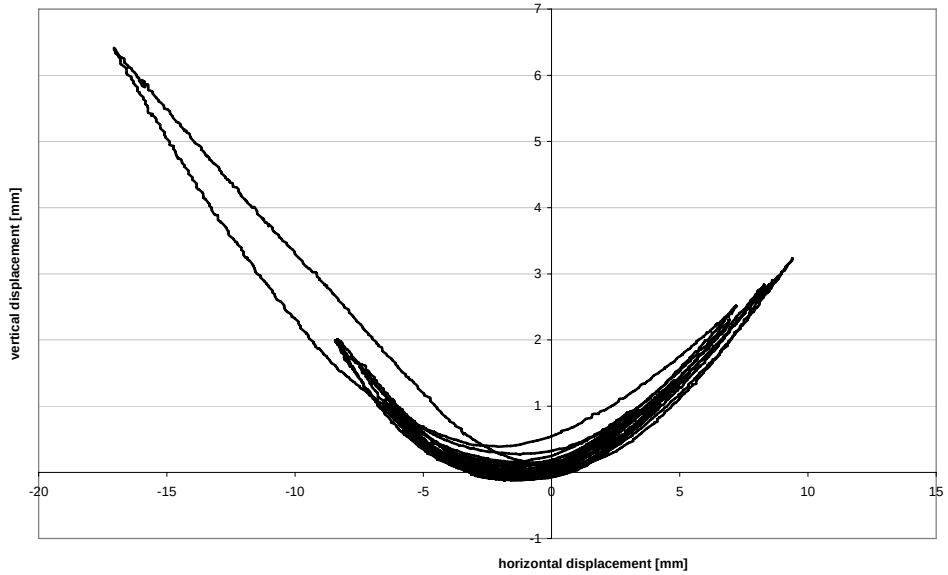

figure A3-9: vertical displacement of wall No.3 (max. 0.32 · g)

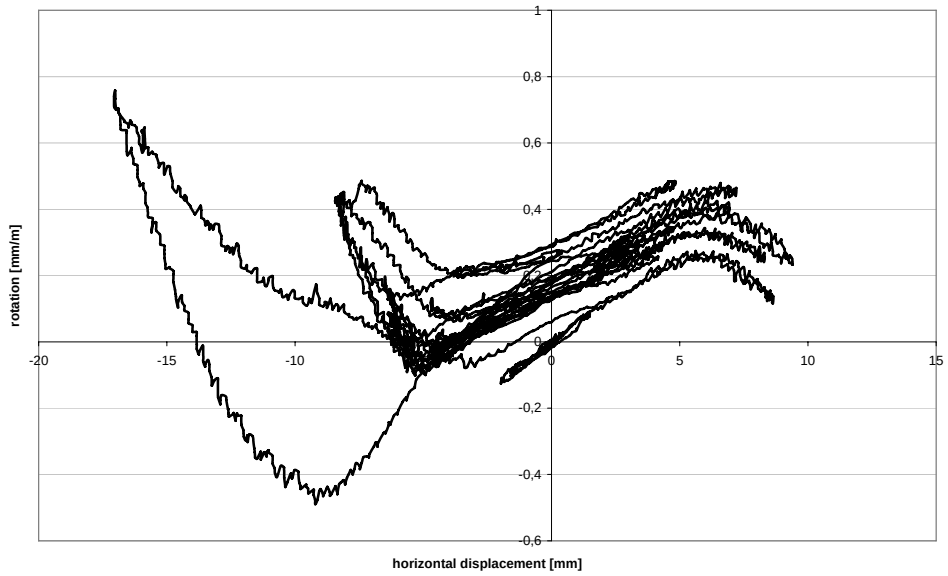

figure A3-10: rotation at the top of wall No.3 (max. 0.32 · g)

figure A4-1: first cracks at about 35 kN of wall No. 4

figure A4-2: crack pattern of wall No. 4 (predamaged)

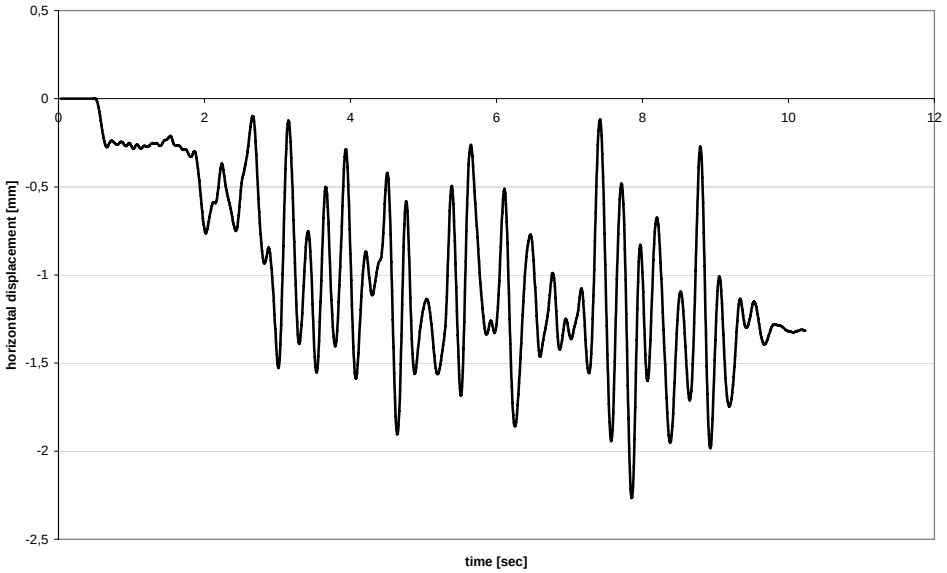

figure A4-3: time history (max. 0.08 · g) of wall No. 4

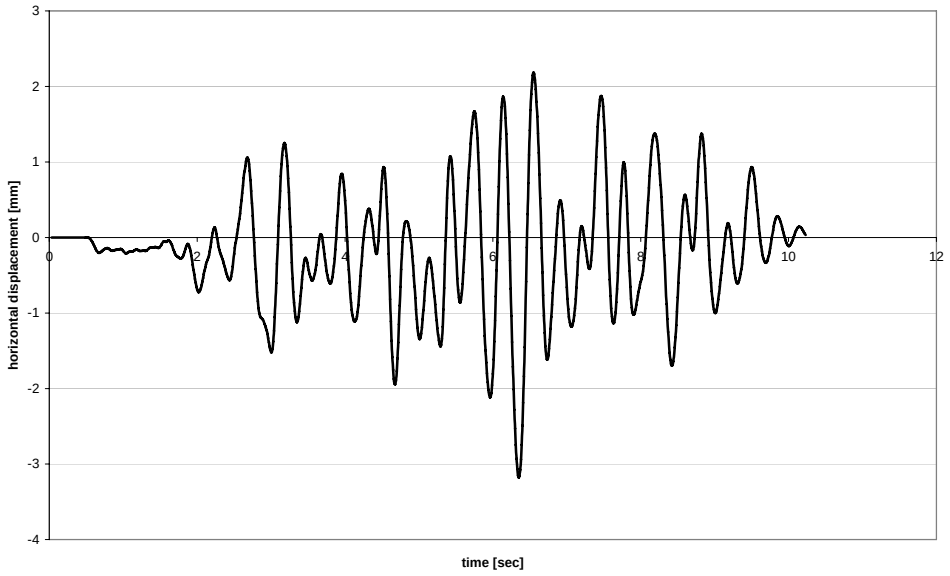

figure A4-4: time history (max. 0.12 · g) of wall No. 4

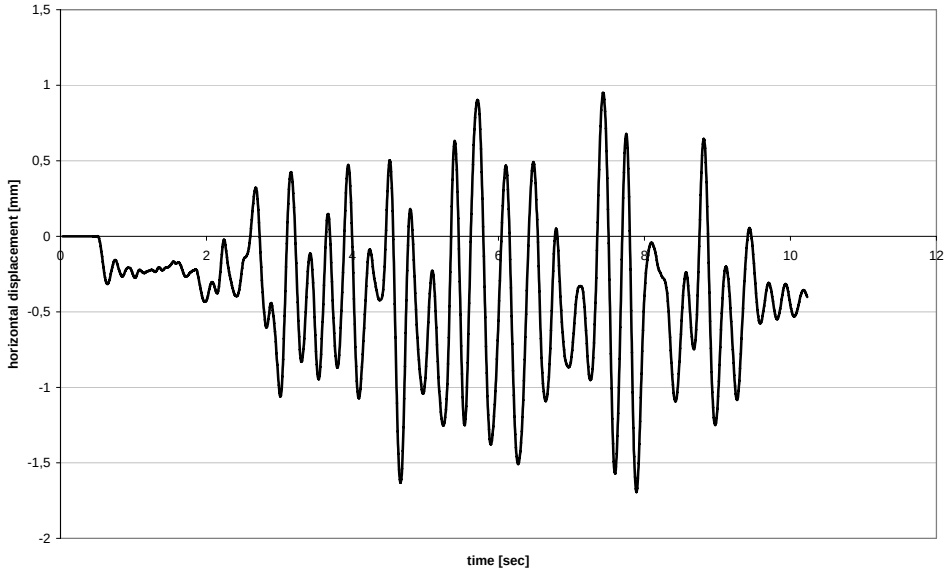

figure A4-5: time history (max. 0.16 · g) of wall No. 4 (predamaged)

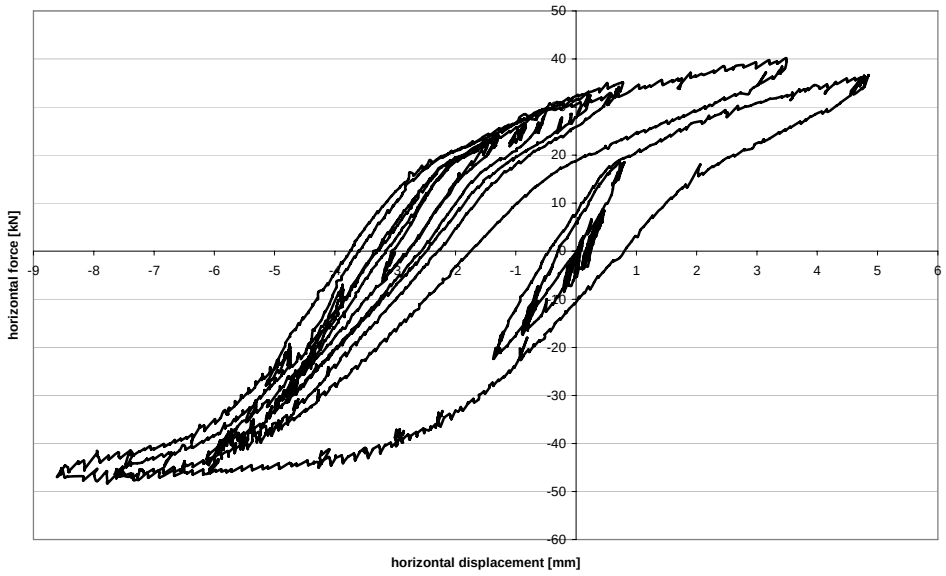

figure A4-6: hysteresis curveof wall No.4 (predamaged / max. 0.16 · g)

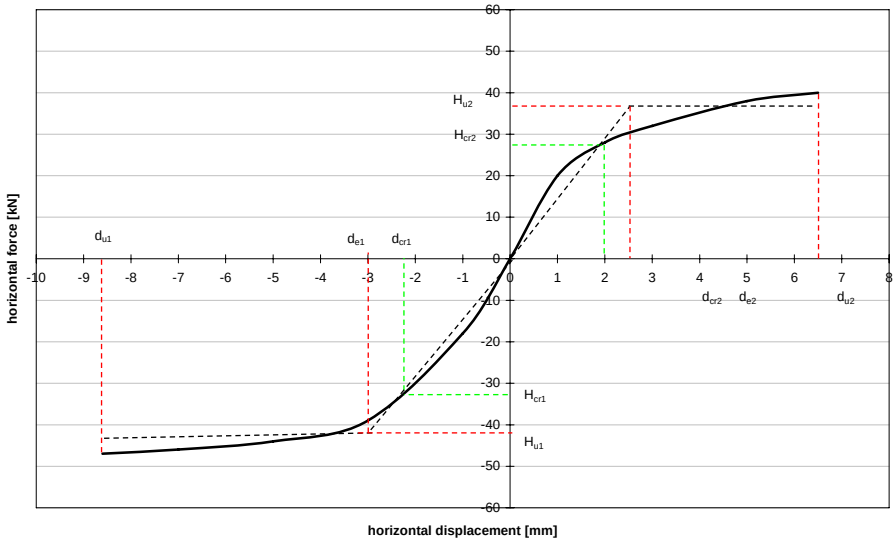

figure A4-7: displaced enveloping curve of wall No.4 (max. 0.16 · g)

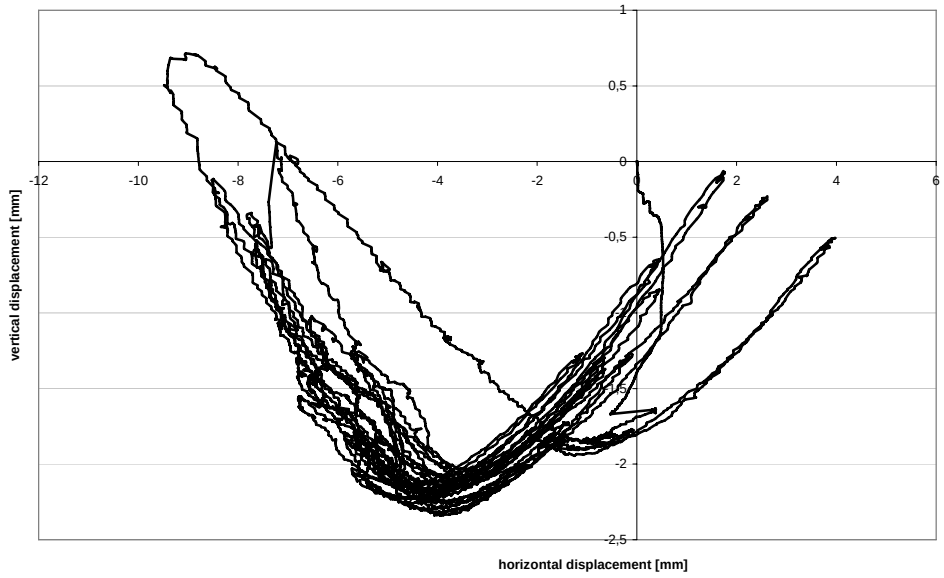

figure A4-8: vertical displacement of wall No.4 (max. 0.16 · g)

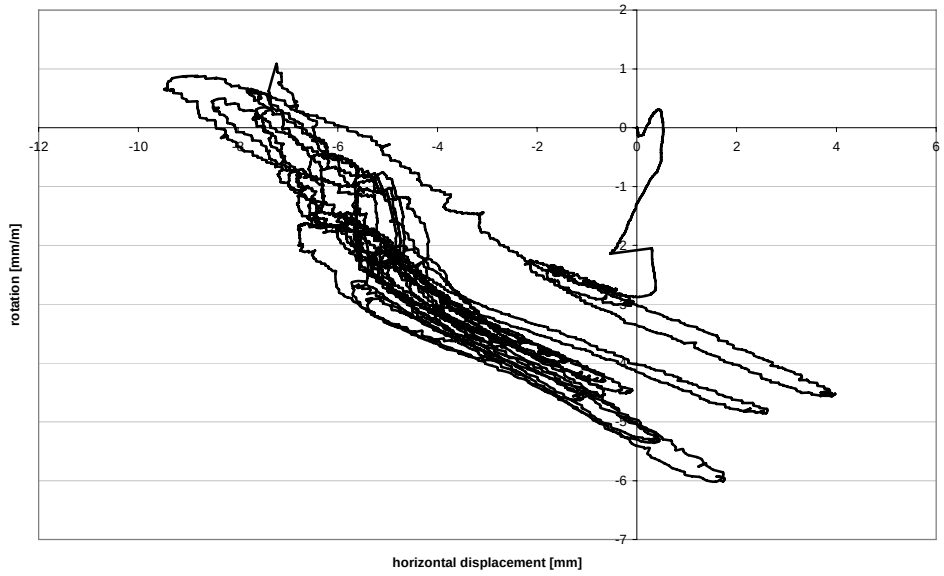

figure A4-9: rotation at the top of wall No.4 (max. 0.16 · g)

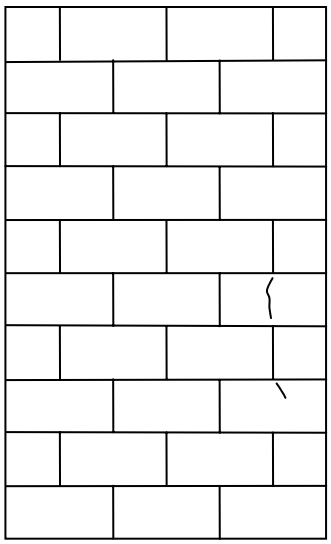

figure A5-1: first cracks at about -38 kN of wall No. 5

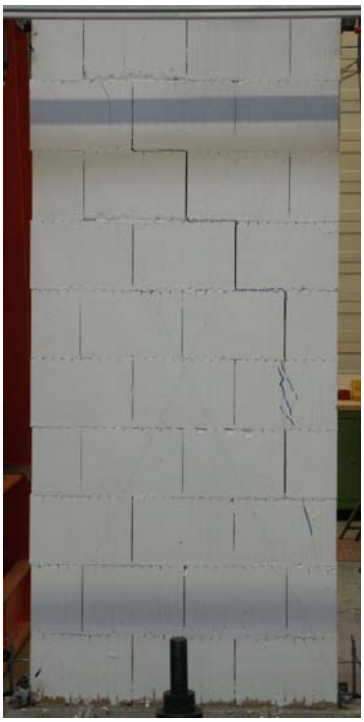

figure A5-2: crack pattern of wall No. 5

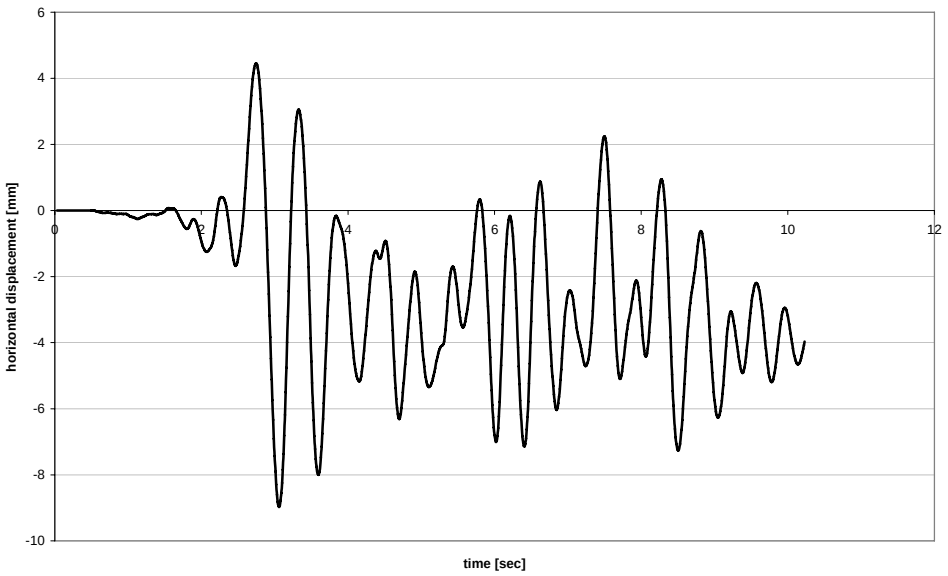

figure A5-3: time history (max. 0.08 · g) of wall No. 5

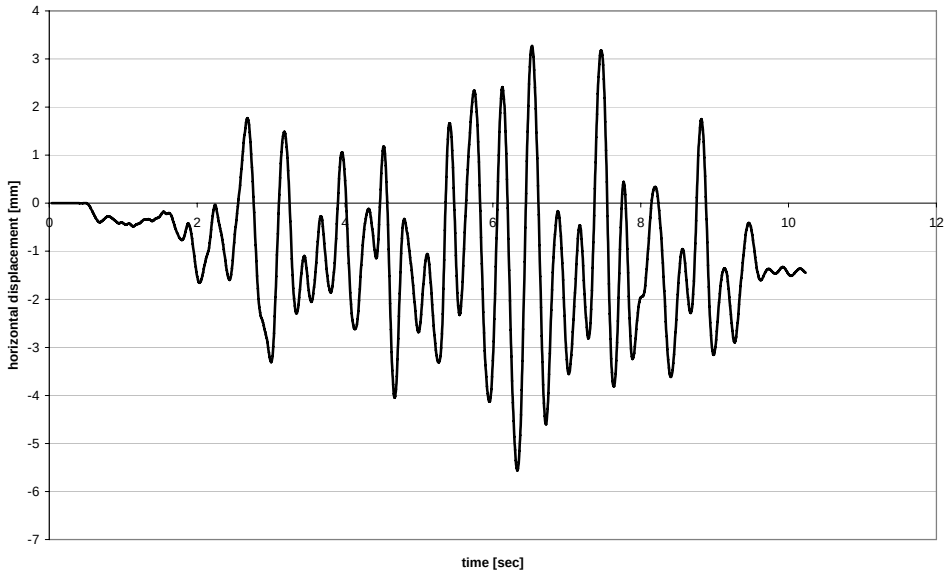

figure A5-4: time history (max. 0.24 · g) of wall No. 5

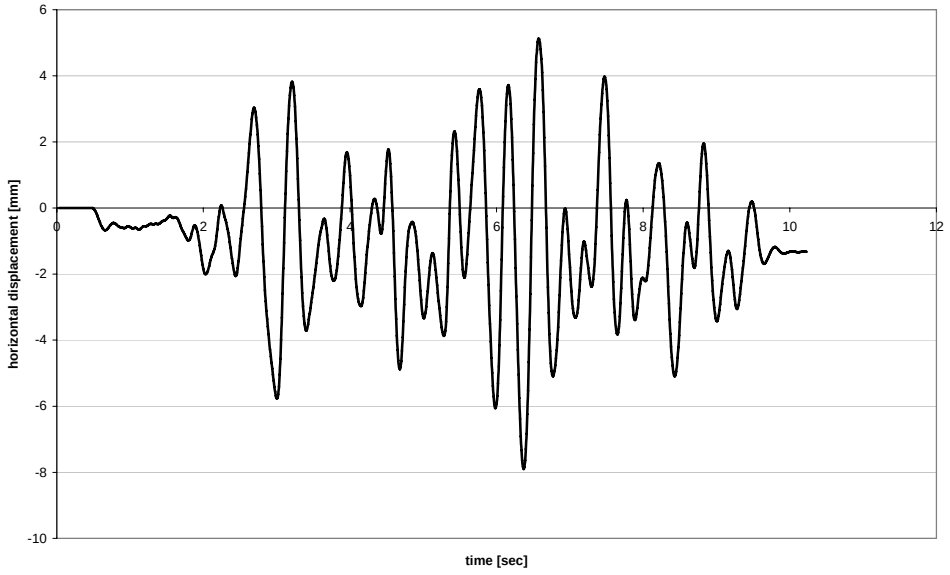

figure A5-5: time history (max. 0.30 · g) of wall No. 5

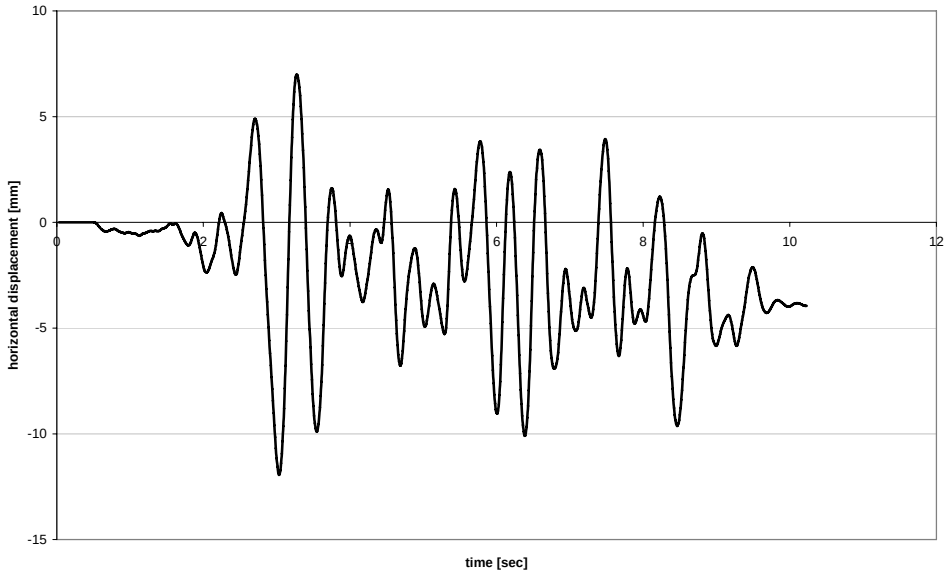

figure A5-6: time history (max. 0.36 · g) of wall No. 5

figure A5-6: hysteresis curveof wall No.5 (max. 0.36 · g)

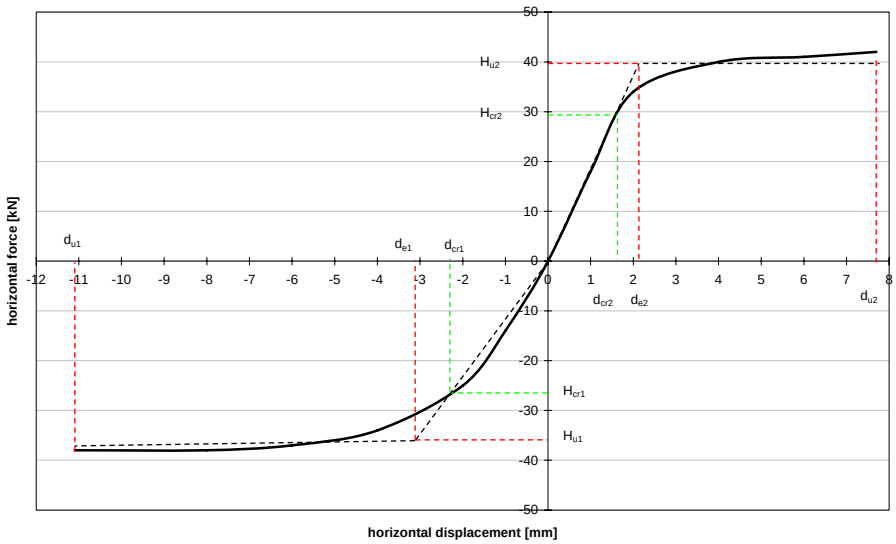

figure A5-7: enveloping curve of wall No.5 (max. 0.36 · g)

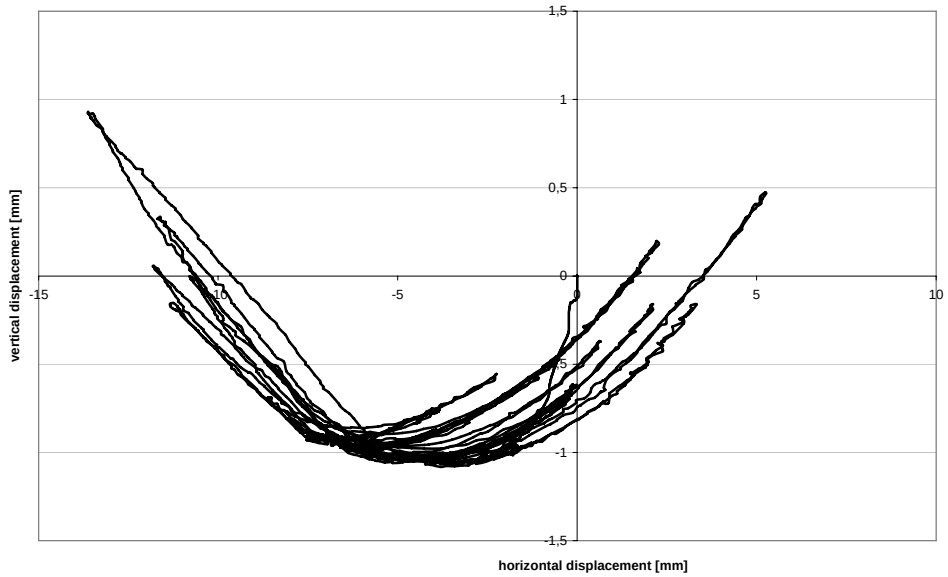

figure A5-8: vertical displacement of wall No.5 (max. 0.36 · g)

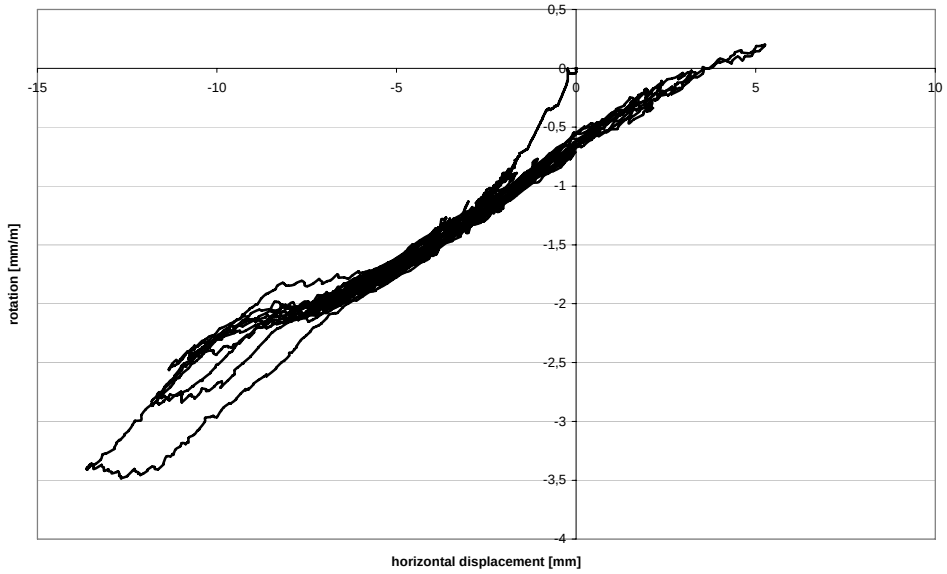

figure A5-9: rotation at the top of wall No.5 (max. 0.36 · g)

figure A6-1: opening of the bed joint of wall No. 6

figure A6-2: opening of the had joint of wall No. 6

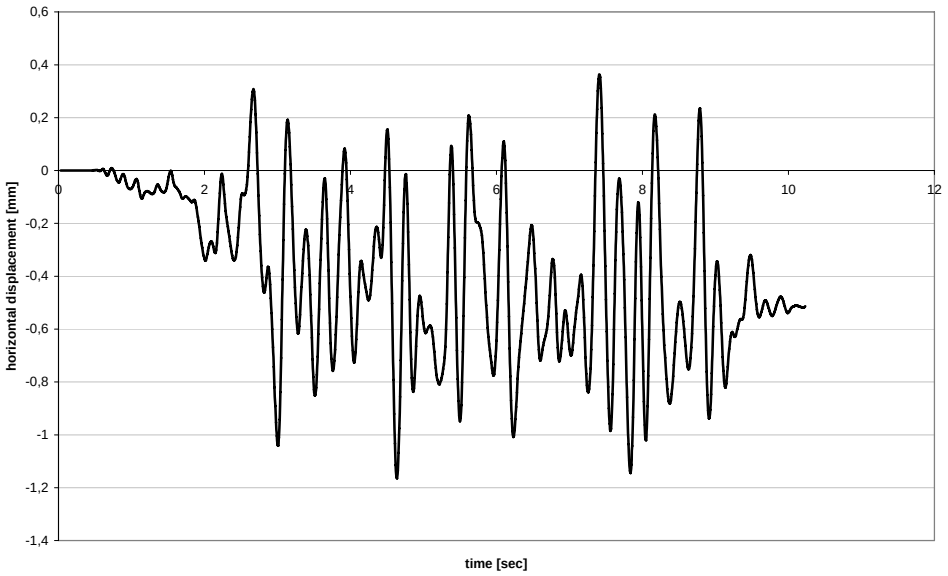

figure A6-3: time history (max. 0.08 · g) of wall No. 6

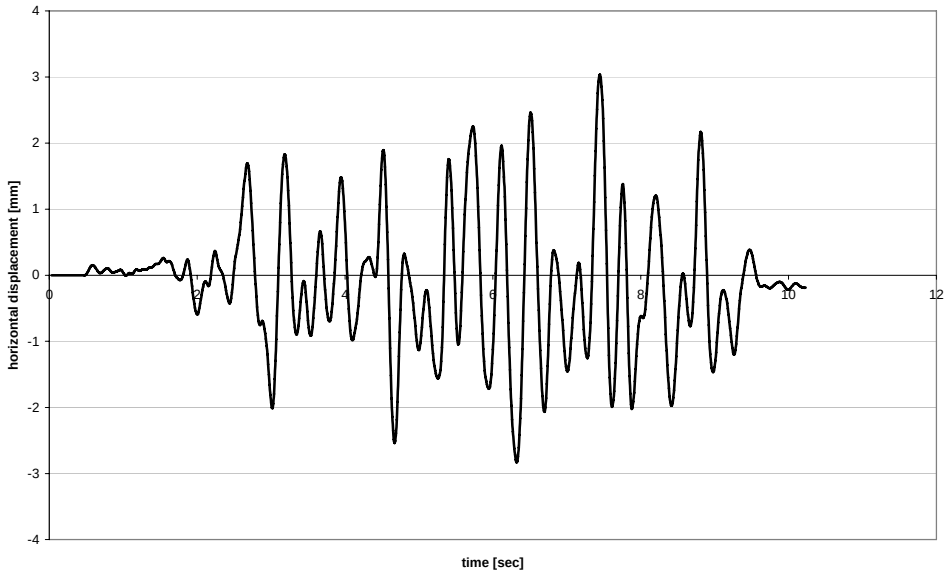

figure A6-4: time history (max. 0.20 · g) of wall No. 6

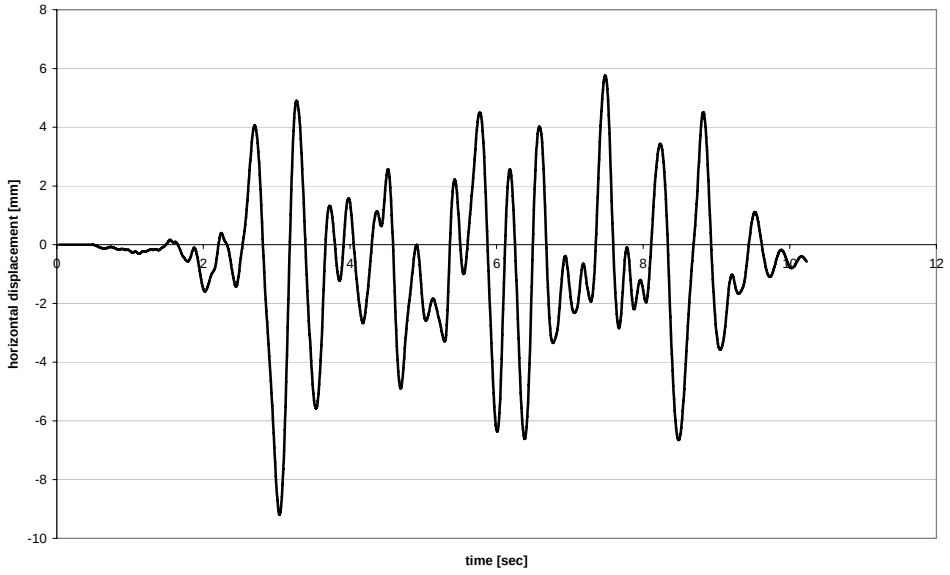

figure A6-5: time history (max. 0.32 · g) of wall No. 6

figure A6-6: hysteresis curveof wall No.6 (max. 0.32 · g)

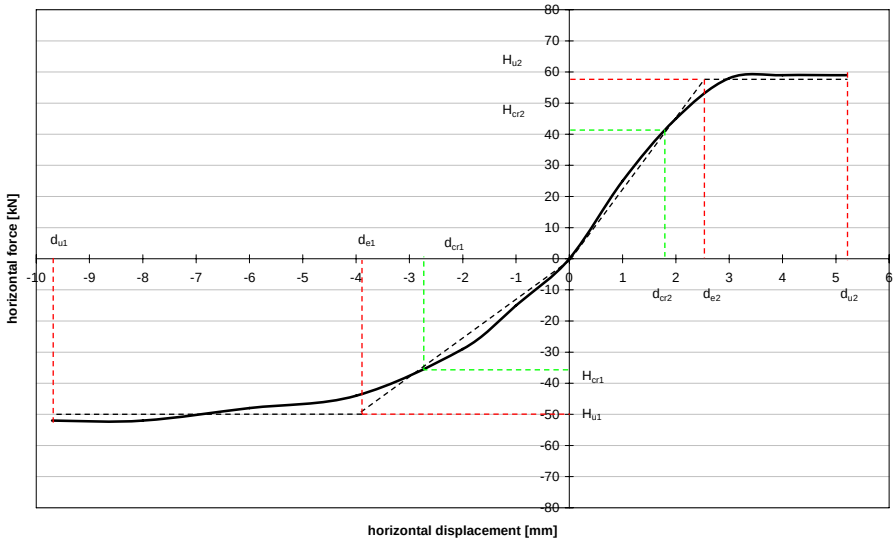

figure A6-7: enveloping curve of wall No.6 (max. 0.32 ·g)

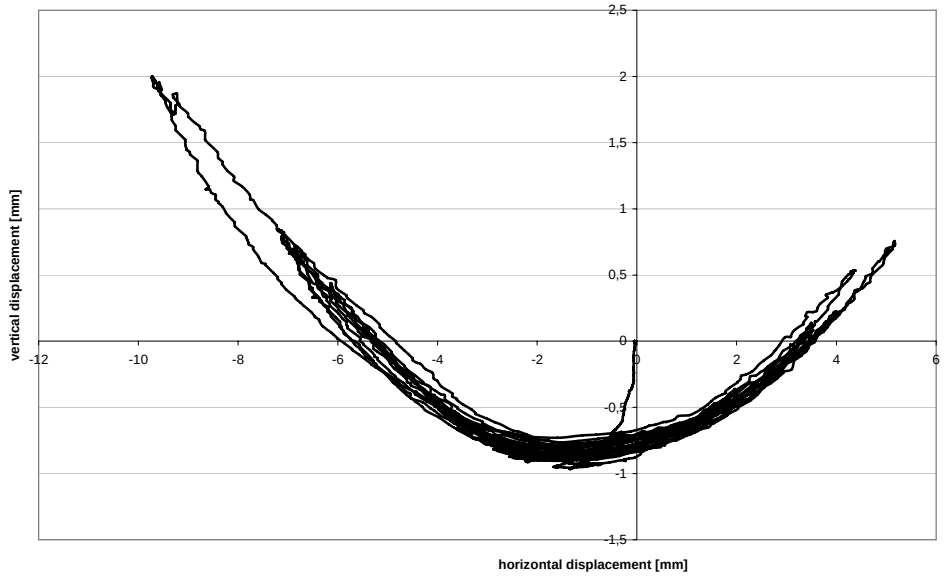

figure A6-8: vertical displacement of wall No.6 (max. 0.32 · g)

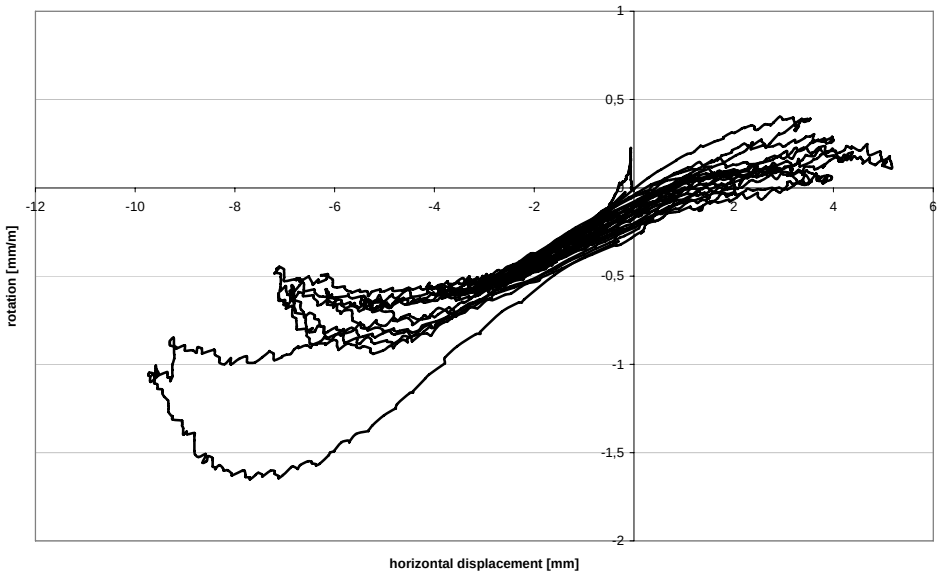

figure A6-9: rotation at the top of wall No.6 (max. 0.32 · g)

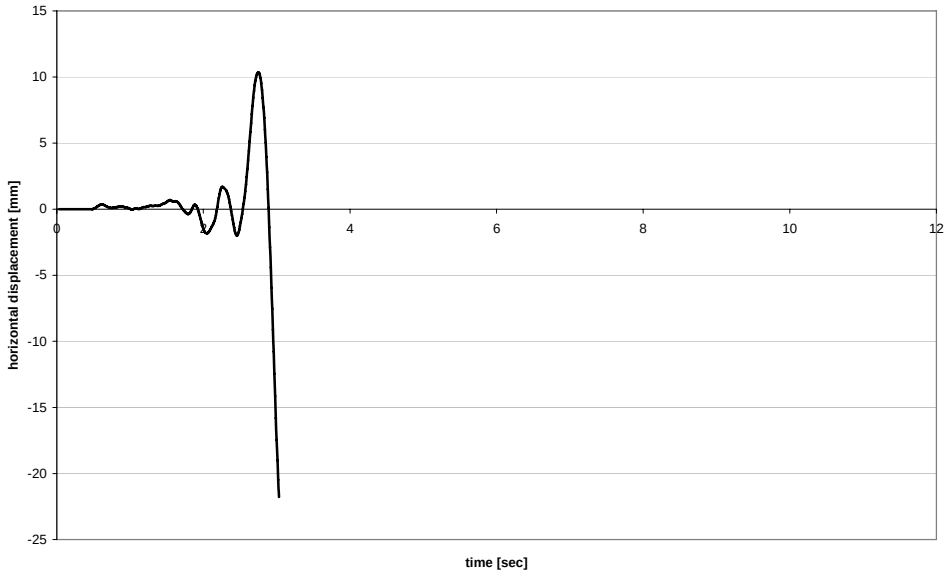

figure A6-10: time history (max. 0.40 · g) of wall No. 6

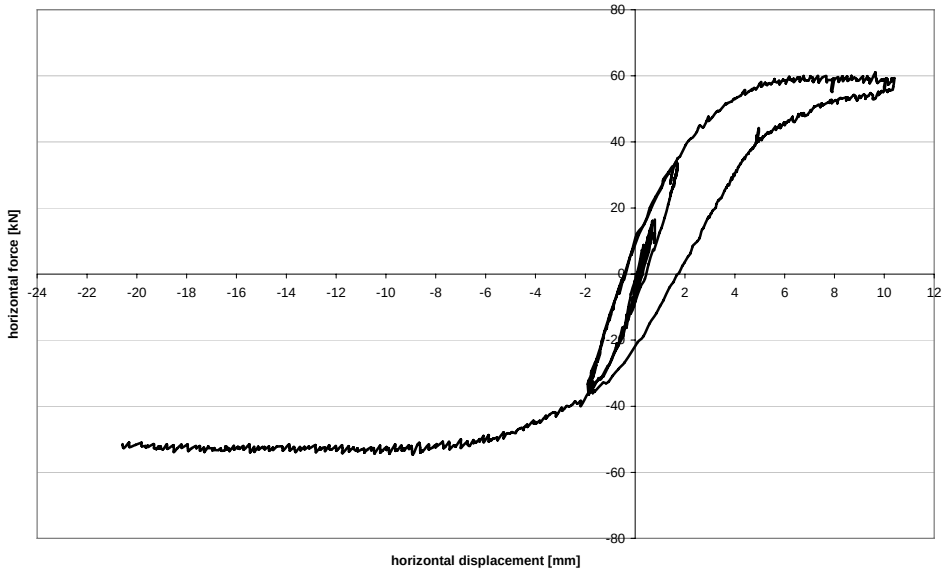

figure A6-11: hysteresis curveof wall No.6 (max. 0.40 · g)

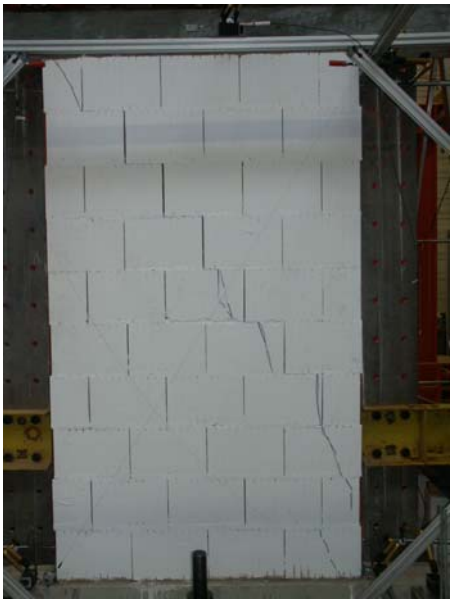

figure A7-1: first cracks at about -50 kN of wall No. 7

figure A7-2: local failure of wall No. 7

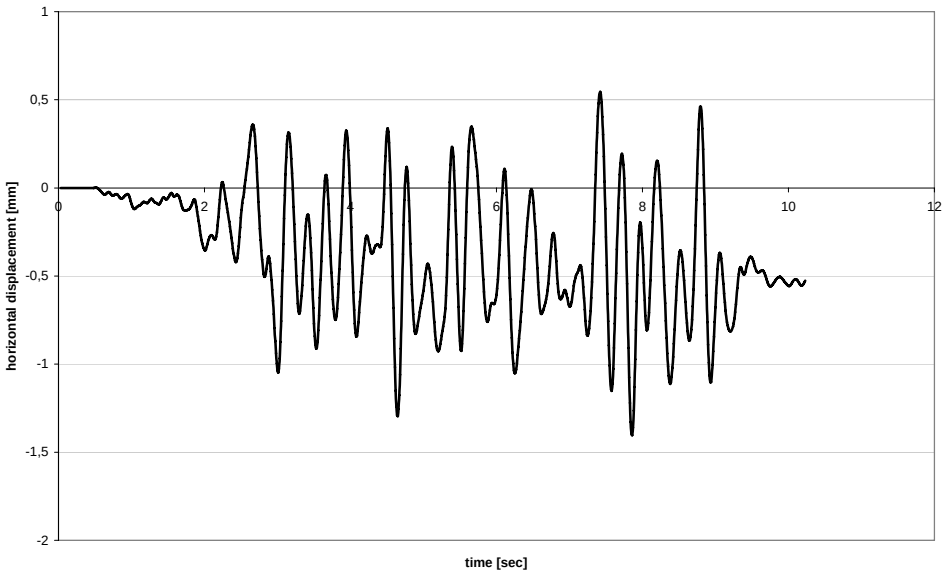

figure A7-3: time history (max. 0.08 · g) of wall No. 7

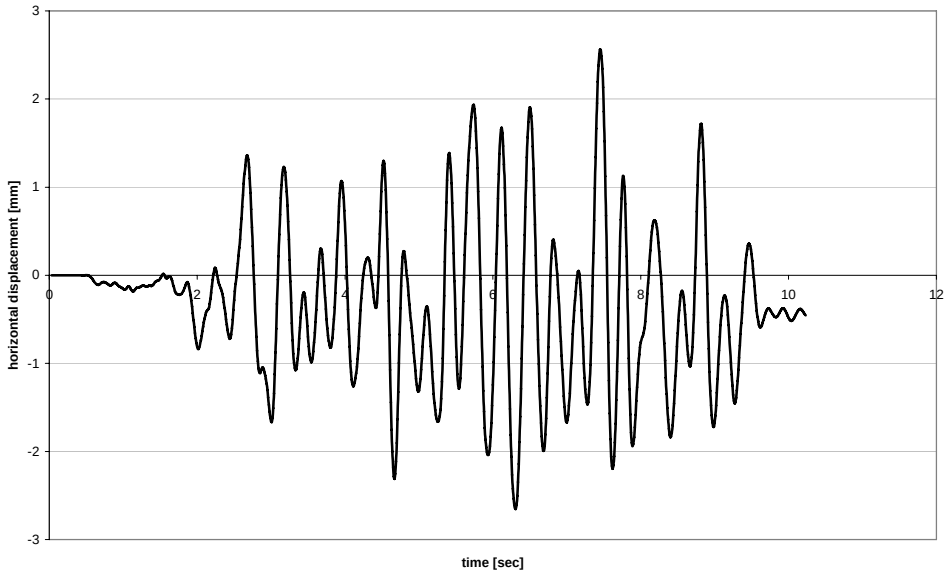

figure A7-4: time history (max. 0.16 · g) of wall No. 7

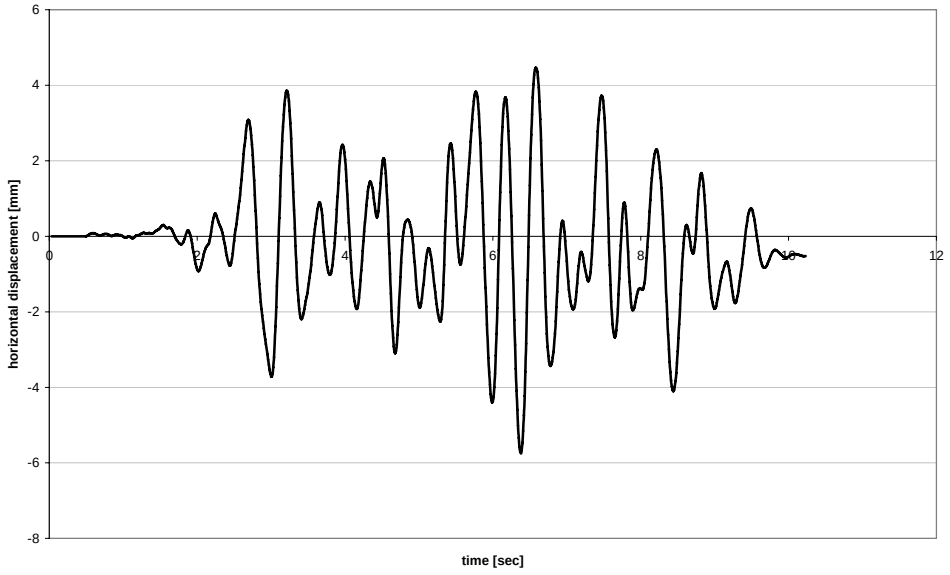

figure A7-5: time history (max. 0.24 · g) of wall No. 7

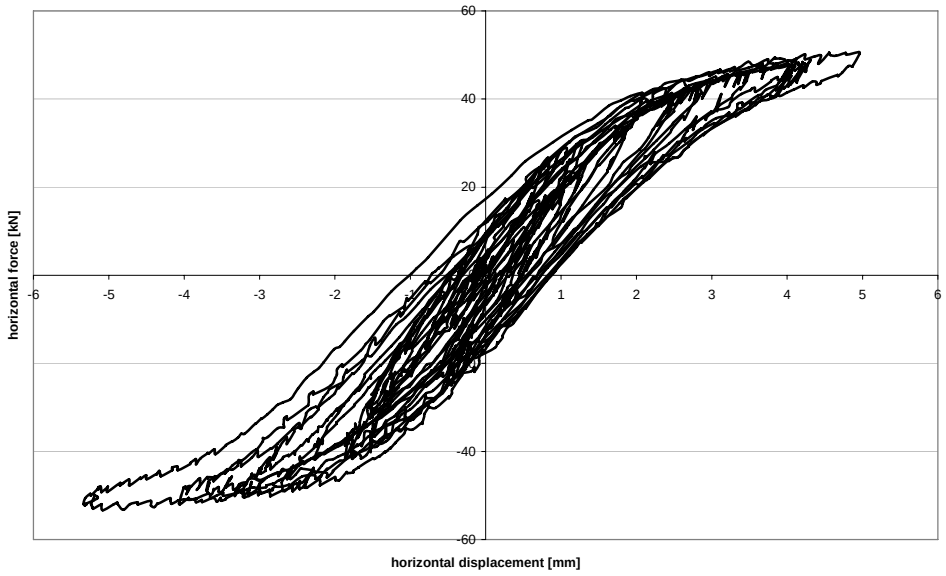

figure A7-6: hysteresis curveof wall No.7 (max. 0.24 · g)

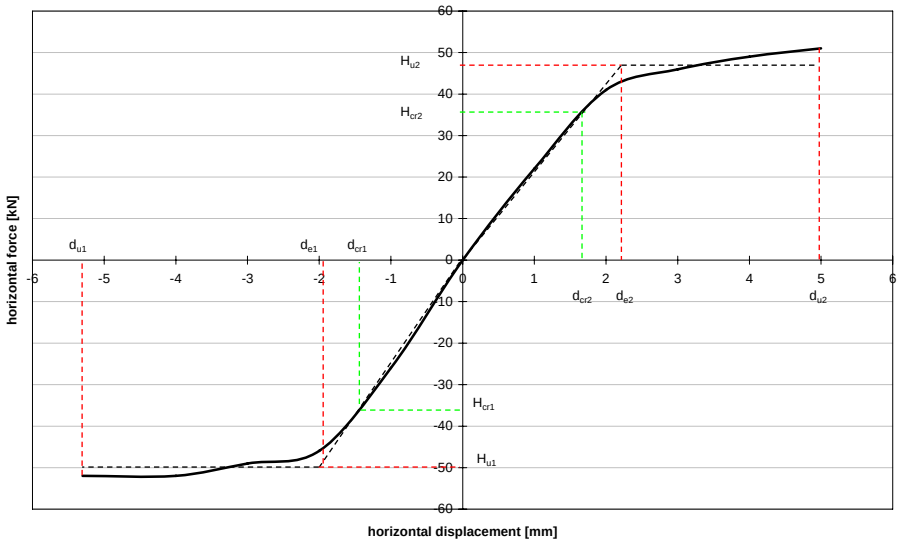

figure A7-7: enveloping curve of wall No.7 (max. 0.24 · g)

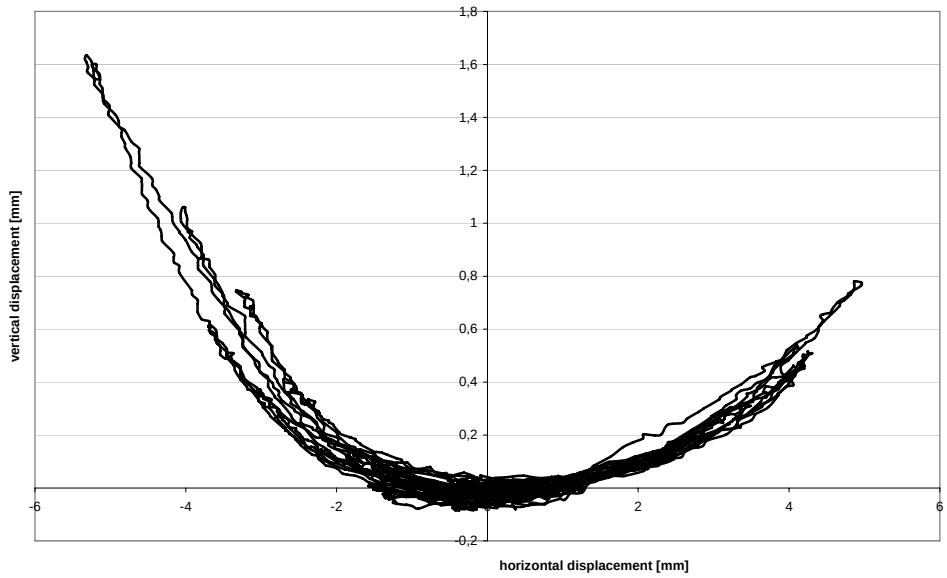

figure A7-8: vertical displacement of wall No.7 (max. 0.24 · g)

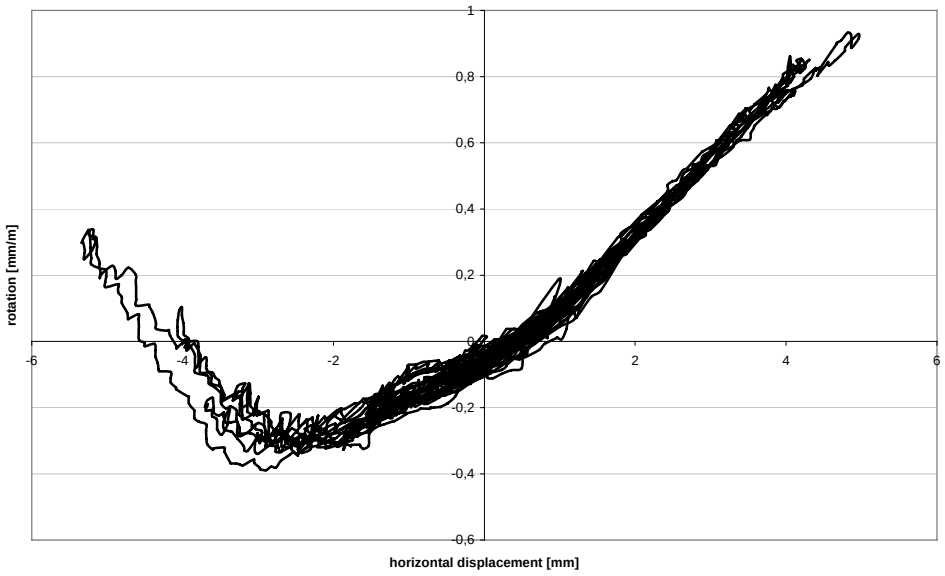

figure A7-9: rotation at the top of wall No.7 (max. 0.24 · g)

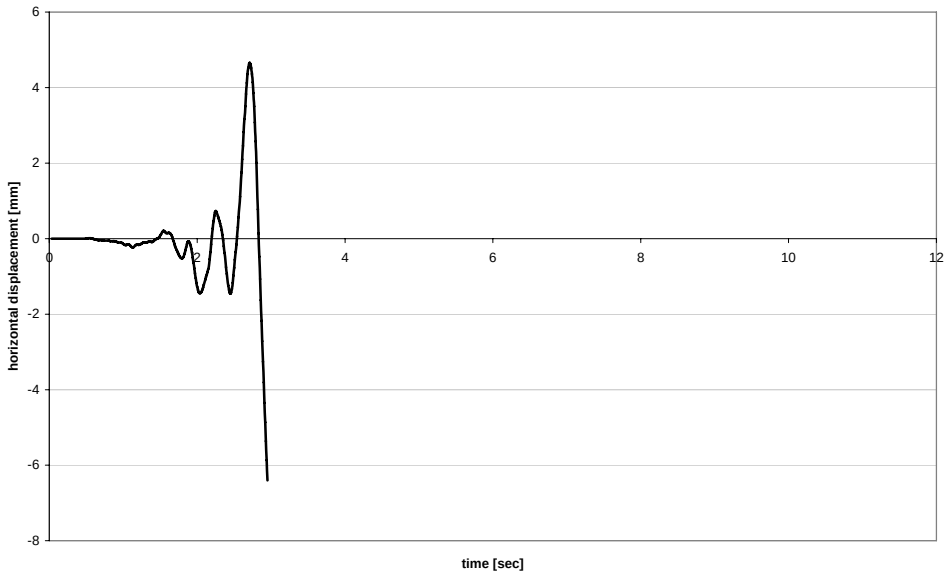

figure A7-10: time history (max. 0.28 · g) of wall No. 7

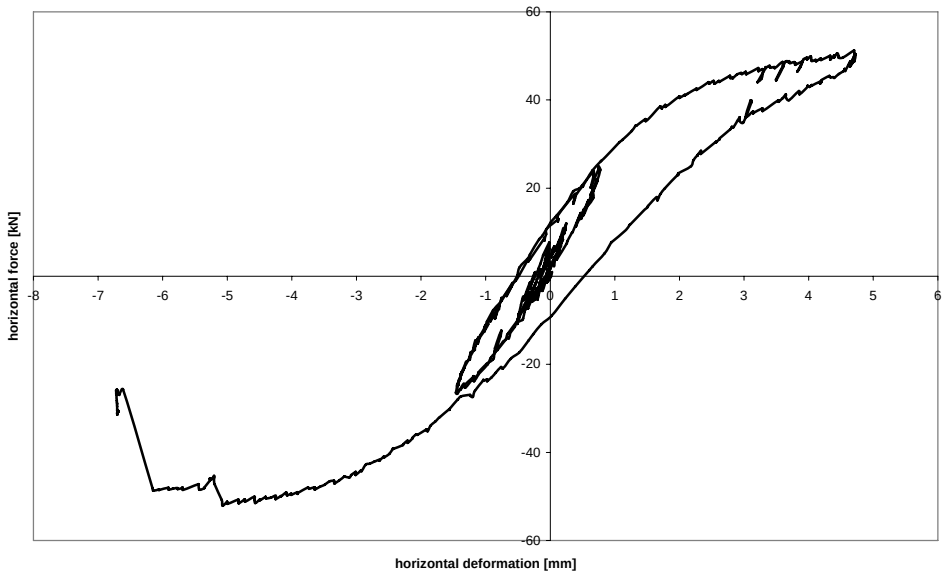

figure A7-11: hysteresis curveof wall No.7 (max. 0.28 · g)

figure A8-1: gaping of the bed joint of wall No. 8

figure A8-2: crack pattern of wall No. 8

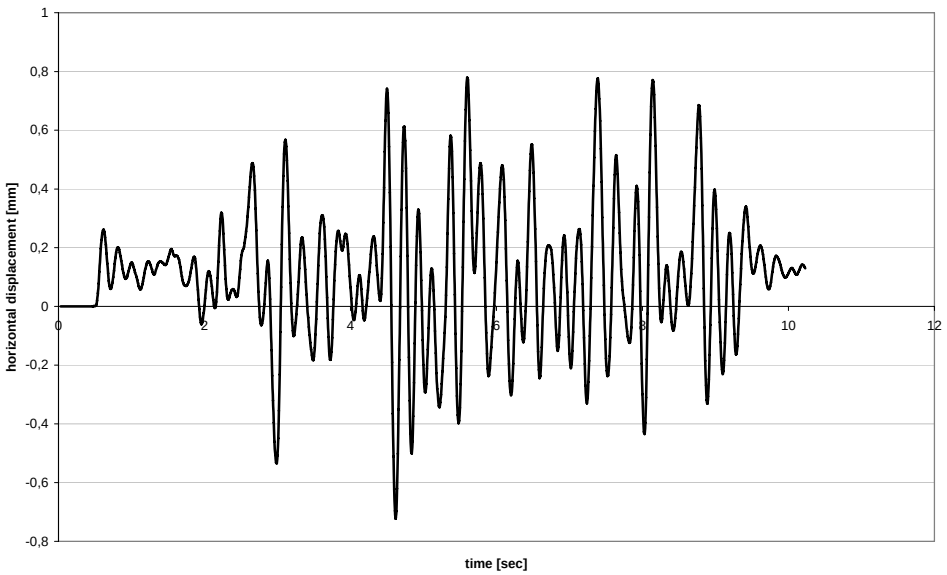

figure A8-3: time history (max. 0.08 · g) of wall No. 8

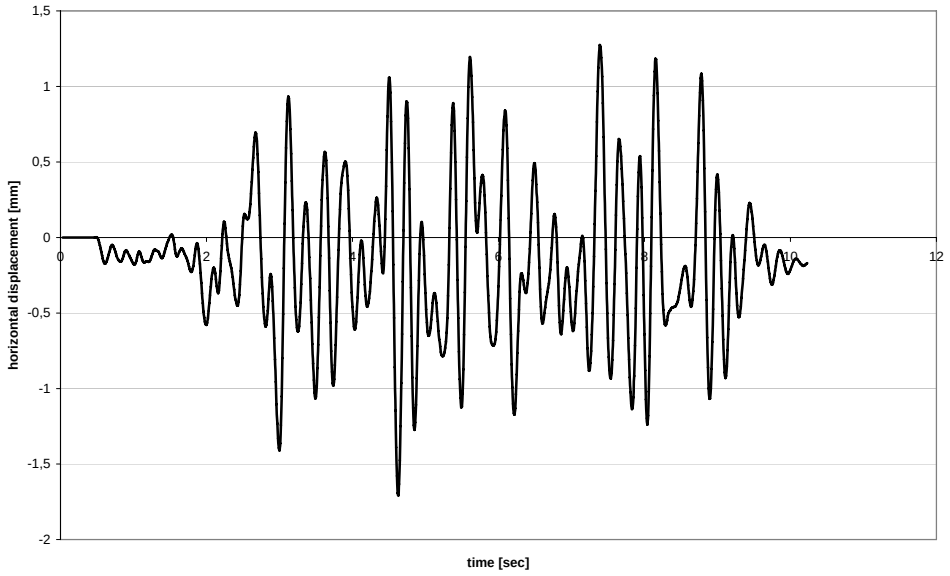

figure A8-4: time history (max. 0.16 · g) of wall No. 8

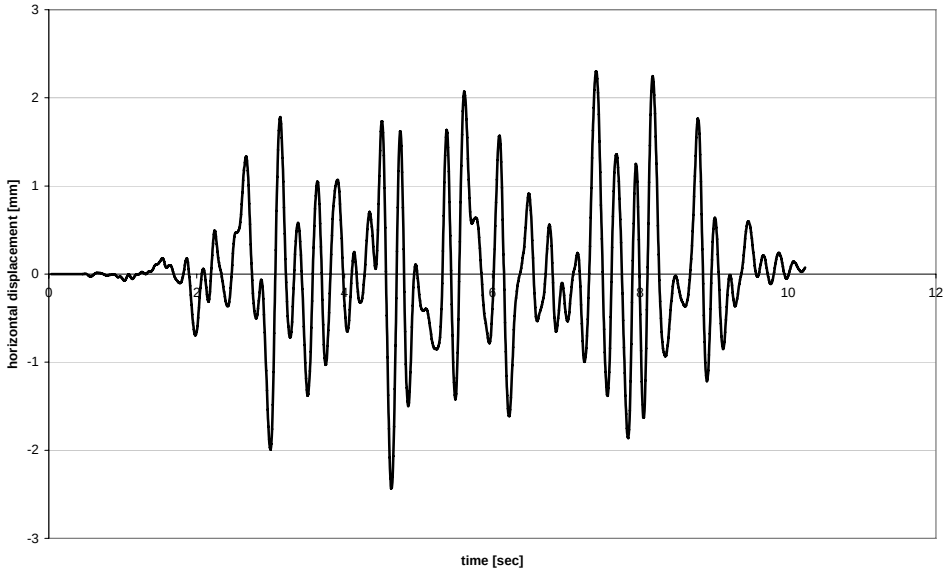

figure A8-5: time history (max. 0.24 · g) of wall No. 8

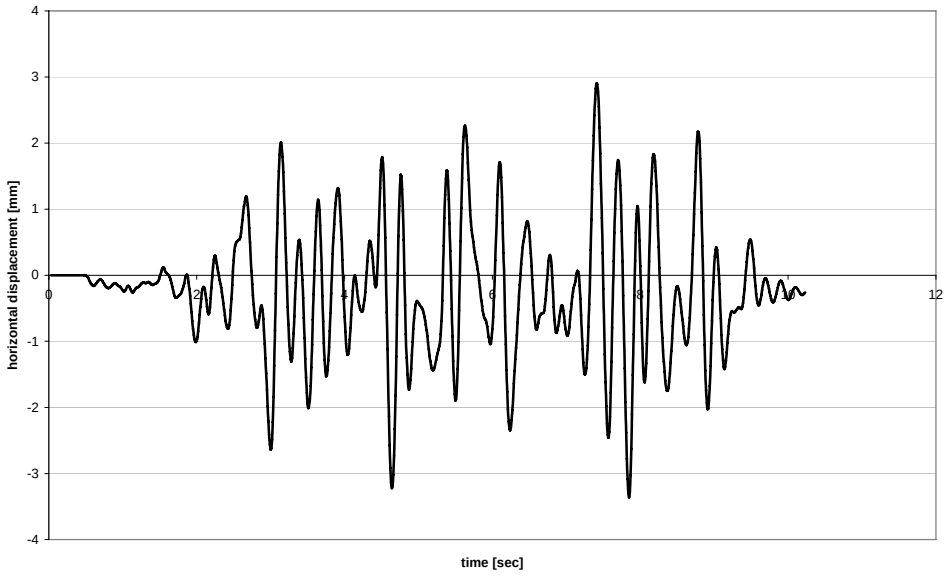

figure A8-6: time history (max. 0.28 · g) of wall No. 8

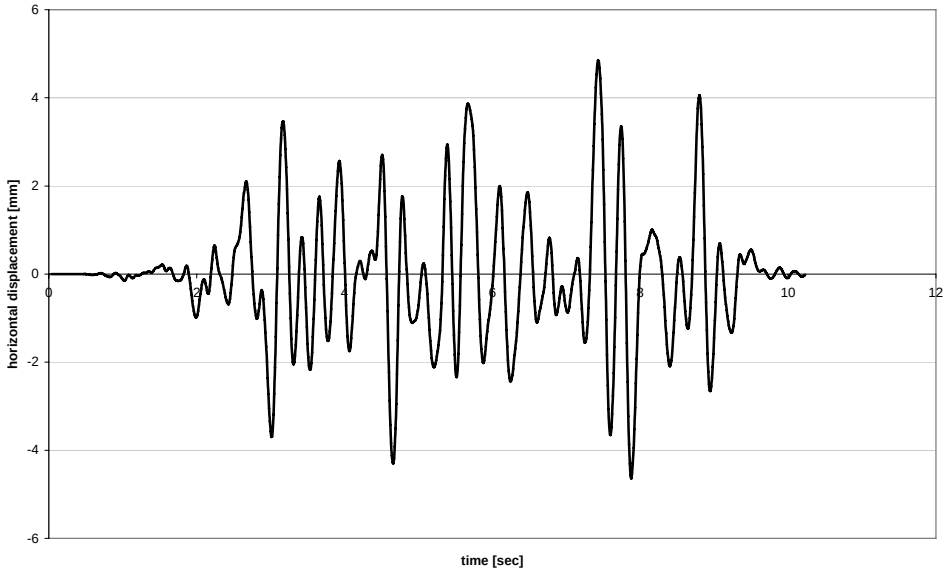

figure A8-7: time history (max. 0.36 · g) of wall No. 8

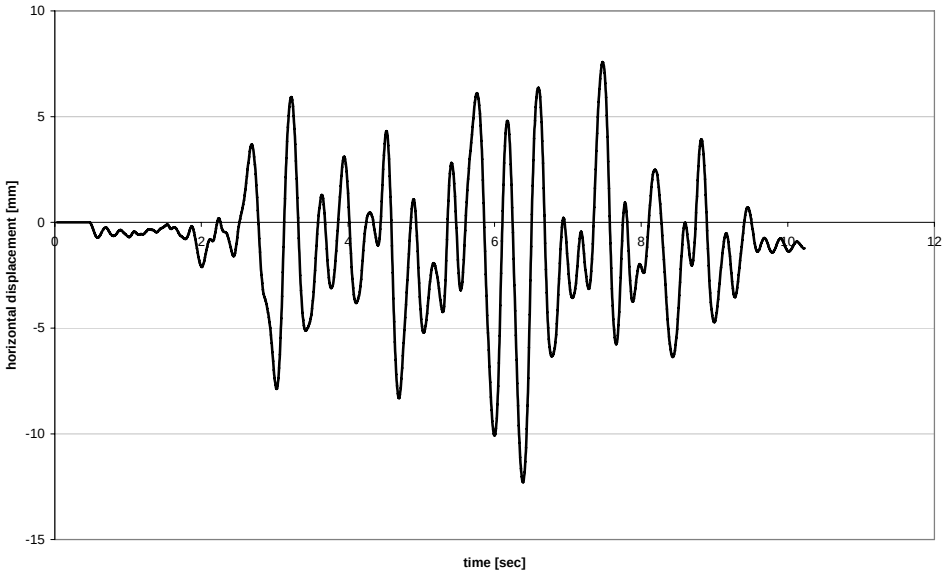

figure A8-8: time history (max. 0.48 · g) of wall No. 8

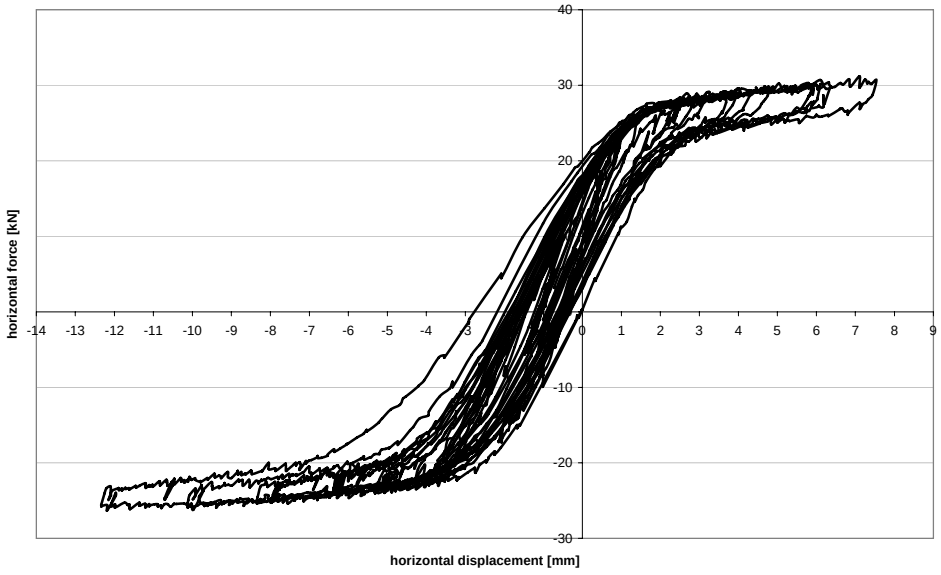

figure A8-9: hysteresis curveof wall No.8 (max. 0.48 · g)

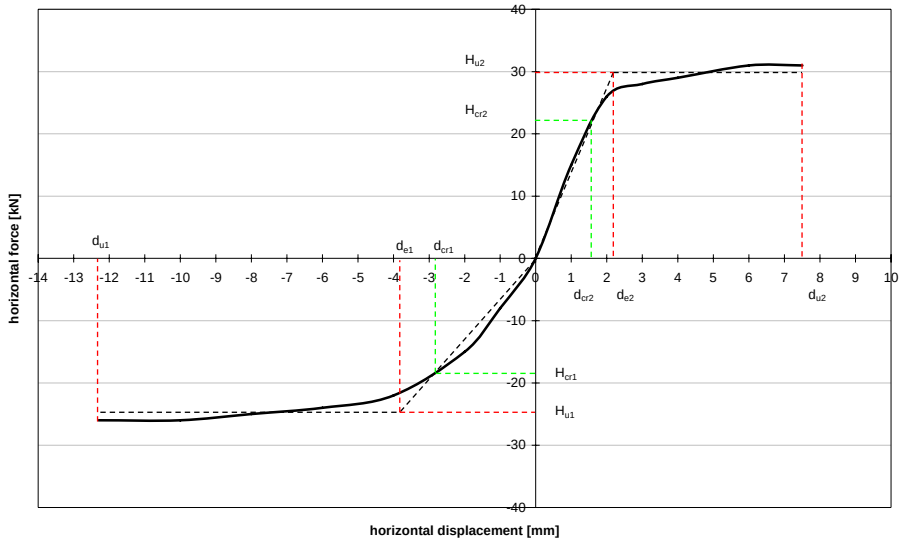

figure A8-10: enveloping curve of wall No.8 (max. 0.48 · g)

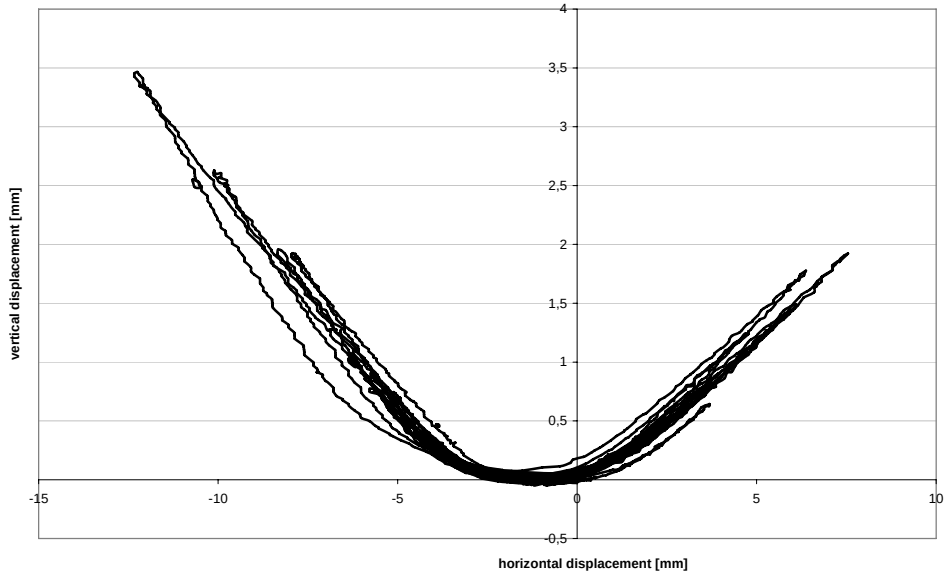

figure A8-11: vertical displacement of wall No.8 (max. 0.48 · g)

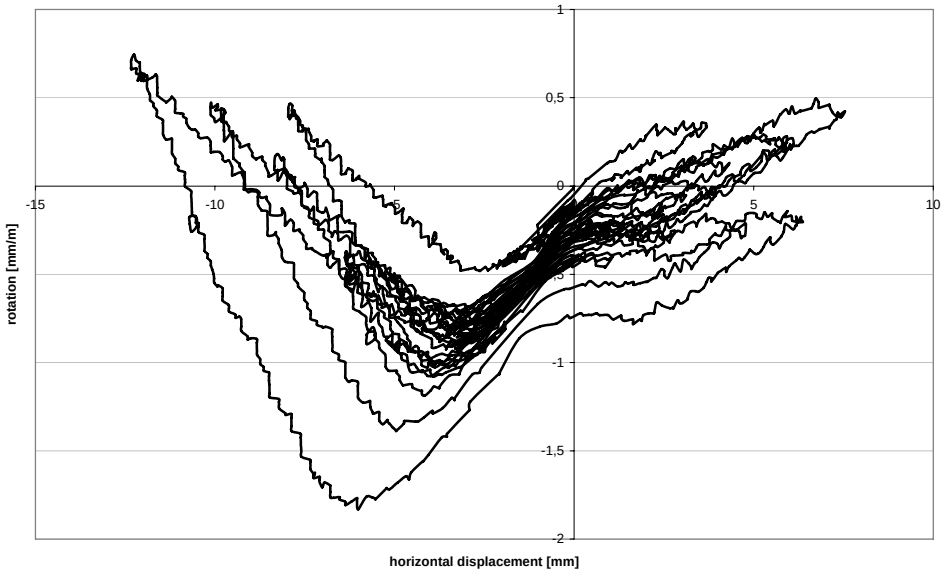

figure A8-12: rotation at the top of wall No. 8 (max. 0.48 · g)